CHEMICAL REVIEWS

REVIEW

pubs.acs.org/CR

Two-Electron Reduced Density Matrix as the Basic Variable in Many-Electron Quantum Chemistry and Physics

David A. Mazziotti*

Department of Chemistry and The James Franck Institute, The University of Chicago, Chicago, Illinois 60637, United States

CONTENTS

1. INTRODUCTION

When Schrödinger[1] derived the now-famous equation bearing his name in 1925, new possibilities emerged for the theoretical and computational prediction of energies and properties of chemical systems and processes. In the 1940s, Eyring, Walter, and Kimball[2] wrote in their introductory book on quantum chemistry that problems in chemistry had been converted by quantum mechanics into problems in applied mathematics. In truth, it would take a long time for advances in both theory and computation to enable accurate predictions of quantum chemical systems. In the 1950s and 1960s, Roothan,[3] Pople,[4] and others solved the Hartree−Fock equations for mean-field energies and properties of atoms and molecules, while in the 1970s and 1980s more sophisticated methods, the coupled cluster method[5] and density functional theory,[6] were designed for the prediction of correlation energies, that is, the differences between the energies from the Hartree−Fock equations and the energies of the many-electron Schrödinger equation. The last 10 years have seen growing interest in the development of electronic structure methods that can treat moderate-to-strong electron correlation, often critical to connecting theoretical predictions and experiments. In this work, we review recent advances in one of these new approaches to the study of electron correlation, the direct calculation of the two-electron reduced density matrix (2-RDM).[7]

In 1951 at a summer conference at Chalk River, the mathematician John Coleman[8] explained to a group of physicists that the many-electron problem might be reducible to only two electrons. Because electrons are indistinguishable with only pairwise interactions, Coleman recognized that the energy of any atom or molecule can be expressed as a linear functional of the 2-RDM.[7,8] This formulation suggested the tantalizing possibility of employing the 2-RDM rather than the many-electron wave function to compute the ground-state energy of an atom or molecule. In 1955, Mayer[9] and Lowdin[10] published similar 2-RDM-based expressions, with Mayer performing a variational calculation. It was soon recognized by Coleman,[8,11] Tredgold,[12] and others, however, that the variational 2-RDM calculations yielded energies that were much too low. The two-electron density matrix had to be constrained to represent a many-electron (or *N*-electron) density matrix (or wave function). Coleman in 1963 called these constraints *N-representability conditions*,[11] and the search for such constraints became known as the *N*-representability problem.

Special Issue: 2012 Quantum Chemistry

Received: February 9, 2011
Published: August 25, 2011

dx.doi.org/10.1021/cr2000493 | *Chem. Rev.* 2012, 112, 244–262

For 40 years, the *N*-representability problem prevented the calculation of the 2-RDM without the many-electron wave function for all but the simplest four-electron systems.[13−15]

In the 1990s, computation of the 2-RDM without the many-electron wave function was achieved by Valdemoro and coworkers,[16−18] Nakatsuji and Yasuda,[19,20] and the author[21−23] through an iterative solution of the contracted Schrödinger equation. Research on the contracted Schrödinger equation had a significant impact on the further development of the variational 2-RDM theory because it led to the recognition that higher-particle RDMs must be invoked for achieving accurate energies and properties in the presence of strong electron correlation. Since then, two complementary approaches to the direct calculation of the 2-RDM have emerged: (i) solution of the contracted Schrödinger equation[16−38] or its anti-Hermitian part[39−55] and (ii) variational minimization of the ground-state energy as a functional of the 2-RDM.[13−15,56−91] Furthermore, in class ii of variational calculations, two approaches to constraining the 2-RDM can be distinguished: (a) the variational 2-RDM methods in which the 2-RDM is constrained by necessary *N*-representability conditions known as positivity conditions[13−15,56−81,92−98] and (b) the *parametric* variational 2-RDM methods in which the 2-RDM is constrained to be nearly *N*-representable by its parametrization.[83−91,99] The collection of these methods has realized a quantum chemistry and physics for molecular systems in which the 2-RDM rather than the many-electron wave function is the basic variable. These 2-RDM methods have been applied to treat moderate and strong correlation in a variety of problems including (i) the conical intersections in methylene[53] and bicyclobutane, (ii) the kinetic stability of oxywater,[99] (iii) the bioluminescence of fireflies,[100] (iv) quantum phase transitions,[101,102] (v) nuclear motion within and beyond the Born−Oppenheimer approximation,[38,79,103] (vi) the metal-to-insulator transition in hydrogen chains,[81] and (vii) the growth of polyradical character with system size in acene chains[80] and sheets.[104] In this work, we develop and review these 2-RDM approaches with an emphasis on their ability to treat moderate-to-strong electron correlation in chemistry and physics.

2. CONTRACTED SCHRöDINGER THEORY

Integration (or contraction in a matrix formulation) of the density-matrix version of the Schrödinger equation over all electrons save two produces the *contracted Schrödinger equation* (CSE).[16−34,36] Section 2.1 presents the CSE as well as its Hermitian (HCSE) and anti-Hermitian (ACSE) parts. If the RDMs in the CSE are *N*-representable, there is a one-to-one mapping between solutions of the Schrödinger equation and solutions of the CSE. The proof of this mapping, first given by Nakatsuji,[105] is presented in second quantization[21] in section 2.2. Nonetheless, neither the CSE nor the ACSE can be solved for the 2-RDM without additional information because these equations depend on higher RDMs. In section 2.3, we discuss the approximate reconstruction of higher RDMs from the 2-RDM to remove the indeterminacy of the CSE and ACSE.[16,21−26,28,29] The practical solution of the ACSE by a system of differential equations[39−53] is outlined in section 2.4, and in section 2.5, we explain recent extensions of the ACSE to treat excited states[50] and arbitrary spin states.[51] Several applications are discussed briefly in the final section.

2.1. Contracted Schrödinger equations

For a quantum *N*-electron system with Hamiltonian $\hat{H}$, the stationary-state energies, E_n, and wave functions, Ψ_n, can be computed from the time-independent Schrödinger equation

$$\hat{H}\Psi_n = E_n\Psi_n \tag{1}$$

or its density-matrix formulation

$$\hat{H}^N D_n = E_n{}^N D_n \tag{2}$$

where the *N*-particle density matrix for the *n*th state is given by ${}^N D_n = \Psi_n\Psi_n^*$. The density-matrix Schrödinger equation can be divided into two separate Hermitian and anti-Hermitian equations:

$$\frac{1}{2}(\hat{H}^N D_n + {}^N D_n\hat{H}) = E_n{}^N D_n \tag{3}$$

$$\frac{1}{2}(\hat{H}^N D_n - {}^N D_n\hat{H}) = 0 \tag{4}$$

Integration of eqs 2, 3, and 4 over the spin and spatial coordinate of electrons 3 to *N* yields the contracted Schrödinger equation (CSE)[16−24,26−34,36]

$$\int \hat{H}^N D_n \, \mathrm{d}3 \ldots \mathrm{d}N = E_n{}^2 D_n \tag{5}$$

as well as the *Hermitian* (HCSE)[27,56,106] and *anti-Hermitian* (ACSE)[39−55] parts of the CSE:

$$\frac{1}{2}\int (\hat{H}^N D_n + {}^N D_n\hat{H}) \, \mathrm{d}3 \ldots \mathrm{d}N = E_n{}^2 D_n \tag{6}$$

$$\frac{1}{2}\int (\hat{H}^N D_n - {}^N D_n\hat{H}) \, \mathrm{d}3 \ldots \mathrm{d}N = 0 \tag{7}$$

The CSE was first obtained in a coordinate representation in 1976 by Cohen and Frishberg[107] and Nakatsuji.[105] The anti-Hermitian part of the CSE (ACSE) was first derived by Harriman[106] in 1979; later in 1979, the ACSE was obtained by Kutzelnigg,[30,108] who called it the generalized Brillouin condition. The ACSE enforces the set of hypervirial relations for all one- and two-body operators, which were developed by Hirshfelder.[109] By definition, the sum of the HCSE and the ACSE produces the CSE. If the Hamiltonian contains at most *pairwise* interactions, both the CSE and the HCSE depend on the 2-, 3-, and 4-RDMs, while the ACSE depends only on the 2- and 3-RDMs.

In a finite basis set, the CSE, as well as the HCSE and ACSE, can be expressed in second quantization as

$$\langle\Psi_n|{}^2\hat{\Gamma}^{i,j}_{k,l}\hat{H}|\Psi_n\rangle = E_n{}^2 D^{i,j}_{k,l} \tag{8}$$

and

$$\frac{1}{2}\langle\Psi_n|\{{}^2\hat{\Gamma}^{i,j}_{k,l},\hat{H}\}|\Psi_n\rangle = E_n{}^2 D^{i,j}_{k,l} \tag{9}$$

$$\frac{1}{2}\langle\Psi_n|[{}^2\hat{\Gamma}^{i,j}_{k,l},\hat{H}]|\Psi_n\rangle = 0 \tag{10}$$

where the operator ${}^2\hat{\Gamma}^{ij}_{k,l}$ is the two-electron *reduced density operator* (2-RDO)

$${}^2\hat{\Gamma}^{i,j}_{k,l} = a_i^\dagger a_j^\dagger a_l a_k \tag{11}$$

each index *i*, *j*, *k*, and *l* denotes a one-electron spin orbital that is a product of a spatial orbital and a spin function σ equal to either

dx.doi.org/10.1021/cr2000493 |*Chem. Rev.* 2012, 112, 244–262

α (+1/2) or β (−1/2), and the elements of the 2-RDM

$$ {}^2D^{i,j}_{k,l} = \langle \Psi_n | a_i^\dagger a_j^\dagger a_l a_k | \Psi_n \rangle \tag{12} $$

follow from the expectation value of the 2-RDO with respect to $|\Psi_n\rangle$. In second quantization, the creation operator $a_i^\dagger$ generates an electron in the ith spin orbital, while the annihilation operator a_k destroys an electron in the kth spin orbital. For a quantum many-electron system, the Hamiltonian is expressible as

$$ \hat{H} = \sum_{p,s} {}^1K^p_s a_p^\dagger a_s + \sum_{p,q,s,t} {}^2V^{p,q}_{s,t} a_p^\dagger a_q^\dagger a_t a_s \tag{13} $$

where the one- and two-electron reduced Hamiltonian matrices ${}^1K$ and ${}^2V$ contain the one- and two-electron integrals, respectively. It will also sometimes be useful to define the Hamiltonian as

$$ \hat{H} = \sum_{p,q,s,t} {}^2K^{p,q}_{s,t} a_p^\dagger a_q^\dagger a_t a_s \tag{14} $$

where ${}^2K$ is the two-electron reduced Hamiltonian

$$ {}^2K^{p,q}_{s,t} = \frac{1}{N-1} {}^1K^p_s \delta^q_t + {}^2V^{p,q}_{s,t} \tag{15} $$

From the definitions of the Hamiltonian and the 2-RDM in eqs 14 and 12, respectively, we can readily express the energy as a linear functional of the two-electron reduced Hamiltonian and the 2-RDM

$$ E = \sum {}^2K^{p,q}_{s,t} {}^2D^{p,q}_{s,t} \tag{16} $$

$$ E = Tr({}^2K\, {}^2D) \tag{17} $$

Furthermore, by rearranging the creation and annihilation operators according to the anticommutation relations for fermions, we can write the CSE and the HCSE in terms of the elements of the 2-, 3-, and 4-RDMs and the ACSE in terms of the elements of the 2- and 3-RDMs. Explicit expressions for these contracted equations in terms of the spin−orbital elements of the reduced Hamiltonians and RDMs are given elsewhere.[7,17,21,30,43]

2.2. Nakatsuji's Theorem

The CSE is an important ingredient for 2-RDM methods because it is a *stationary-state condition for both ground and excited states*.[21,50,105] By Nakatsuji's theorem, if the RDMs in the CSE are N-representable, then for energetically nondegenerate states, both ground and excited states, there is a one-to-one mapping between the solutions of the Schrödinger equation and solutions of the CSE.[21,105] The above derivation clearly proves that the SE implies the CSE. To complete the proof of Nakatsuji's theorem, we need to prove that the CSE implies the SE. While early work[18,20] on the CSE assumed that Nakatsuji's theorem,[105] proven in 1976 for the integro-differential form of the CSE, remains valid for the *second-quantized* CSE in a finite orbital basis set, the author first presented the following formal proof in 1998.[21]

The SE equation can be satisfied if and only if

$$ \langle \psi | \hat{H}^2 | \psi \rangle - \langle \psi | \hat{H} | \psi \rangle^2 = 0 \tag{18} $$

known as the dispersion condition. Multiplying both sides of the CSE in eq 8 by the reduced Hamiltonian elements ${}^2K^{i,j}_{k,l}$ and summing over the remaining indices produces

$$ \langle \psi | \Big(\sum_{i,j;k,l} {}^2K^{i,j}_{k,l} a_i^\dagger a_j^\dagger a_l a_k \Big) \Big(\sum_{p,q;s,t} {}^2K^{p,q}_{s,t} a_p^\dagger a_q^\dagger a_t a_s \Big) | \psi \rangle = E \Big(\sum_{i,j;k,l} {}^2K^{i,j}_{k,l} {}^2D^{i,j}_{k,l} \Big) \tag{19} $$

The sum on the right-hand side of the above equation is equal to the energy E, and from eq 14, we realize that the sums on the left-hand side are just Hamiltonian operators in the second-quantized notation. Hence, when the 2-RDM corresponds to an N-particle wave function ψ, eq 22 implies eq 18, and the proof of Nakatsuji's theorem is accomplished.

Because the Hamiltonian is defined in second quantization, the proof of Nakatsuji's theorem is also valid when the one-particle basis set is incomplete. While an exact Nakatsuji-like theorem has not been proven for the ACSE, the ACSE implies a significant part of the CSE.[50] Unlike the SE, the CSE only requires the 2- and 4-RDMs in the given one-particle basis rather than the full N-particle wave function. Despite their importance as stationary-state conditions, neither the CSE nor the ACSE can be solved for the 2-RDM without additional information because they both depend on higher-particle RDMs.

2.3. Cumulant Reconstruction of RDMs

A significant advance occurred in the 1990s when it was recognized that the indeterminacy of these equations could be removed by *reconstructing the higher RDMs as functionals of the 2-RDM*.[16,19,21,22] In 1993, Colmenero, Pérez del Valle, and Valdemoro[16] introduced a set of reconstruction functionals based on particle−hole duality, and in 1996, Nakatsuji and Yasuda[19] confirmed these functionals by Green's function techniques. In 1998, Mazziotti[21,22] systematized and generalized these reconstructions by developing a *cumulant theory for RDMs*.[22,24,26,28] Cumulant reconstruction of RDMs has been applied to solving both the CSE[16,19,21] and ACSE.[39−55]

Both the 3- and 4-RDMs can be expressed as follows:[22−26,28,110]

$$ {}^3D^{p,q,s}_{t,u,v} = +6\,{}^1D^p_t \wedge {}^1D^q_u \wedge {}^1D^s_v + 9\,{}^2\Delta^{p,q}_{t,u} \wedge {}^1D^s_v + {}^3\Delta^{p,q,s}_{t,u,v} \tag{20} $$

and

$$ {}^4D^{p,q,s,t}_{u,v,y,z} = +24\,{}^1D^p_u \wedge {}^1D^q_v \wedge {}^1D^s_y \wedge {}^1D^t_z + 72\,{}^2\Delta^{p,q}_{u,v} \wedge {}^1D^s_y \wedge {}^1D^t_z + 24\,{}^2\Delta^{p,q}_{u,v} \wedge {}^2\Delta^{s,t}_{y,z} + 16\,{}^3\Delta^{p,q,s}_{u,v,y} \wedge {}^1D^t_z + {}^4\Delta^{p,q,s,t}_{u,v,y,z} \tag{21} $$

where the 3- and 4-RDMs are normalized, as in second quantization, to $N!/(N-3)!$ and $N!/(N-4)!$, ${}^1D$ is the 1-RDM, and ${}^2\Delta$, ${}^3\Delta$, and ${}^4\Delta$ are the cumulant (or connected) parts of the 2-, 3-, and 4-RDMs. Importantly, both the 1-RDM and the cumulant part of a p-RDM scale *linearly* with system size r, whereas, in contrast, the p-RDM scales as r^p.[7,22,23,26,29] Furthermore, the cumulant p-RDM vanishes until the $(p-1)$th order of a renormalized perturbation theory.[7,22,23,26,29] The symbol ∧ denotes the antisymmetric tensor product known as the *Grassmann (or wedge) product*.[21,111]

dx.doi.org/10.1021/cr2000493 |*Chem. Rev.* 2012, 112, 244–262

To eliminate the 3-RDM from the CSE or ACSE approximately, we can *reconstruct* the 3-RDM from the 2-RDM according to its *cumulant expansion*[22,24,26,29,28,110]

$$ {}^3D^{p,q,s}_{t,u,v} \approx 6\,{}^1D^p_t \wedge {}^1D^q_u \wedge {}^1D^s_v + 9\left({}^2D^{p,q}_{t,u} - 2\,{}^1D^p_t \wedge {}^1D^q_u\right) \wedge {}^1D^s_v \quad (22) $$

where $\wedge$ denotes the antisymmetric Grassmann (or wedge) product.[21,111] The missing term in the reconstruction, known as the connected (or cumulant) part ${}^3\Delta$ of the 3-RDM, contains information not expressible as wedge products of the 1- and 2-RDMs.[22,24,26,28,29,110] Although the connected 3-RDM can be approximated in terms of the 2-RDM, it is neglected in the multireference formulation of the ACSE in ref 45. Solution of the CSE also requires reconstruction of the 4-RDM, which can be accomplished by a similar approximation of its cumulant expansion.[18−22,24,26−34,36]

The cumulant reconstruction[22,24,26,28] is also an essential part of the canonical transformation (CT) method,[112,113] which has been shown to be a solution of the ACSE in the Heisenberg representation.[41] Despite their theoretical connections, the ACSE and CT methods are practically very different with distinct fundamental variables (the 2-RDM (ACSE) versus an effective Hamiltonian (CT)), convergence behaviors, results, and capabilities.[41,48] In general, reconstruction is an important component of any method within contracted Schrödinger theory, that is, a theory using the CSE or a part of the CSE, such as the ACSE, as a stationary-state condition.[50]

2.4. Solving the ACSE

In this section, we combine the ACSE and the cumulant reconstruction of the 3-RDM from the 2-RDM from the previous sections to solve the ACSE for the 2-RDM. Consider a sequence of infinitesimal two-body unitary transformations of an initial wave function $\Psi(\lambda)$

$$ |\Psi(\lambda + \epsilon)\rangle = \mathrm{e}^{\epsilon\hat{S}(\lambda)}|\Psi(\lambda)\rangle \quad (23) $$

where the transformations are ordered by a continuous time-like variable λ. For the transformation to be unitary, the two-body operator $\hat{S}$, defined by

$$ \hat{S}(\lambda) = \sum_{p,q,s,t} {}^2S^{p,q}_{s,t}(\lambda)\,{}^2\hat{\Gamma}^{p,q}_{s,t} \quad (24) $$

must be *anti-Hermitian*, $\hat{S}^\dagger = -\hat{S}$. The operator $\hat{S}(\lambda)$ can be chosen to minimize the energy along the path defined by λ.

As shown in refs 39, 41, 42, and 45, the following differential equations for the changes of the energy and its 2-RDM with λ are obtained from eq 23 by letting $\epsilon \rightarrow 0$:

$$ \frac{\mathrm{d}E}{\mathrm{d}\lambda} = \langle\Psi(\lambda)|[\hat{H}, \hat{S}(\lambda)]|\Psi(\lambda)\rangle \quad (25) $$

and

$$ \frac{\mathrm{d}^2D^{i,j}_{k,l}}{\mathrm{d}\lambda} = \langle\Psi(\lambda)|[{}^2\hat{\Gamma}^{i,j}_{k,l}, \hat{S}(\lambda)]|\Psi(\lambda)\rangle \quad (26) $$

To minimize the energy along λ, we select the following elements of the two-particle matrix ${}^2S^{p,q}_{s,t}(\lambda)$, which minimize $\mathrm{d}E/\mathrm{d}\lambda$ along its gradient with respect to these elements:[73]

$$ {}^2S^{p,q}_{s,t}(\lambda) = -\langle\Psi(\lambda)|[\hat{H}, {}^2\hat{\Gamma}^{p,q}_{s,t}]|\Psi(\lambda)\rangle \quad (27) $$

Importantly, the right side of eq 27 is simply the negative of the residual of the ACSE. If the residual in the ACSE vanishes, the unitary transformations become the identity operator, and the energy and 2-RDM cease to change with λ. Using the cumulant reconstruction of the 3-RDM in eq 22 permits us to express these equations approximately in terms of the 2-RDM. Hence, eqs 25, 26, and 27 collectively provide a system of differential equations[39,41,42,45] for evolving an initial 2-RDM to a final 2-RDM that solves the ACSE for stationary states. In practice, the equations are evolved in λ until either (i) the energy or (ii) the least-squares norm of the ACSE increases. The ACSE can be seeded with an initial 2-RDM from either (i) a Hartree−Fock calculation or (ii) any correlated calculation (i.e., a multiconfiguration self-consistent-field (MCSCF) calculation[45]). Convergence to the ACSE's solution is efficient in both cases.[39,41,45]

Seeding the ACSE with an MCSCF 2-RDM yields a balanced treatment of both single- and multireference correlation.[45,48,50−52] Because the ACSE with reconstruction incorporates many high orders of a renormalized perturbation theory, its energies are significantly more accurate than those from second or third orders of a multireference many-body perturbation theory.[45,48,50,51] Furthermore, in the absence of strong correlation, the ACSE can be compared with coupled cluster methods where it yields energies that are between the accuracies of coupled cluster with single and double excitations (CCSD) and coupled cluster with single, double, and triple excitations (CCSDT).[42] In addition to its balance of moderate and strong correlation effects, the ACSE has advantages in computational scaling. It scales like r^6 where r is the rank of the one-electron basis set, but its accuracy is between that of CCSD and CCSDT where the latter scales as r^7. Moreover, while multireference wave function methods scale *exponentially* with the number r_a of active orbitals, the ACSE only scales *quadratically*, ${r_a}^2$.[45,48] This significant reduction in computational cost allows the ACSE to treat larger active spaces than traditional wave function methods.

2.5. Excited States and Arbitrary Spin States

As demonstrated in the recent extension of the ACSE to excited states,[50] even though the unitary rotations are selected in eq 27 to minimize the energy, the system of differential equations in eqs 25, 26, and 27 is capable of producing energy and 2-RDM solutions of the ACSE for both ground and excited states. Because excited states correspond to local energy minima of the ACSE and the gradient in eq 27 leads to a *local* rather than global energy minimum, an excited-state solution can be readily obtained from a good guess for the initial 2-RDM. A guess will be good when it is closer to the minimum of the desired solution of the ACSE than to any other minimum. Such 2-RDM guesses can be generated from multiconfiguration self-consistent-field (MCSCF) calculations. The initial MCSCF 2-RDM directs the optimization of the ACSE to a desired excited state because it contains important multireference correlation effects that identify the state.

The ACSE method has also recently been extended to treat arbitrary spin states.[51] This extension was achieved through a spin-coupling technique that for arbitrary spin states preserves the efficient matrix blocking of singlet-state 2-RDMs. In the approach, we couple a high-spin molecule to one or more hydrogens at "infinite" separation to yield a composite closed-shell system. Importantly, the noninteracting hydrogens can be added without decreasing the point-group symmetry of the high-spin molecule. Consider, for example, a molecule in a doublet spin state $\psi_n^{1/2,\pm 1/2}$ to which we couple an exact hydrogen wave function at "infinity" $\phi^{1/2,\mp 1/2}$. By standard angular momentum

dx.doi.org/10.1021/cr2000493 |Chem. Rev. 2012, 112, 244–262

coupling techniques, we can write the composite singlet wave function as

$$\Psi_n^{0,0}(1 \ldots N+1) = \frac{1}{\sqrt{2}}(\psi_n^{1/2,+1/2}(1 \ldots N) \wedge \phi^{1/2,-1/2}(N+1) - \psi_n^{1/2,-1/2}(1 \ldots N) \wedge \phi^{1/2,+1/2}(N+1)) \quad (28)$$

The resulting supermolecule is in a singlet state that can be readily treated with the ACSE. This spin-coupling technique, generalizable to arbitrary spin states,[51] has been demonstrated to yield a size extensive (i.e., separable) 2-RDM for high-spin systems of interest.[51]

2.6. Applications

Applications of the ACSE to the ground state have been made to a number of systems and reactions including (i) the electrocyclic ring-opening of bicyclobutane to *gauche*-1,3-butadiene,[47] (ii) the relative energies of the *cis*−*trans* isomers of HO_3^-,[44] (iii) the sigmatropic shift of hydrogen in propene and acetone enolate,[48] (iv) the study of vinylidene carbene reactions,[52] and (v) the photoexcited reaction of allyl radical to cyclopropyl radical.[55] These calculations demonstrate that the ACSE yields a balanced description of single- and multireference (strong) correlation effects in both the presence and absence of strong electron correlation. In contrast, traditional wave function methods tend to be optimal in either the presence (multireference perturbation methods) or absence (coupled-cluster methods) of strong correlation. An equally accurate description of correlation in both limits is extremely important in practical applications where energy differences must be computed between molecular species or states with significantly different degrees of electron correlation.

2.6.1. Energy Barriers of Bicyclobutane's Transition States. In the ring opening of bicyclobutane to *gauche*-1,3-butadiene the energy barrier for the disrotatory pathway includes the energy of a strongly correlated biradical transition state.[47] The ACSE method enables the direct calculation of multireference correlation energies and 2-RDMs without the fully correlated many-electron wave function. Qualitatively, the Woodward−Hoffmann rules indicate that the electrocyclic reaction of bicyclobutane to form *gauche*-1,3-butadiene prefers the conrotatory pathway to the disrotatory pathway. The solution of the ACSE in the 6-311G** basis set predicts 41.2 and 55.7 kcal/mol reaction barriers for the conrotatory and disrotatory pathways, respectively (Figure 1). The ACSE energy barrier of 55 kcal/mol appears to resolve a 10 kcal/mol energy discrepancy between coupled cluster and multireference perturbation methods in the literature.[47]

2.6.2. Excited and Arbitrary-Spin States. Because excited states generally contain more multireference correlation than ground states, the ACSE method is especially applicable to treating both the energies and properties of excited states. In 2009, the ACSE methodology was extended to treat both excited states[50] and arbitrary spin states.[51] Initial benchmark calculations included the excited states of hydrogen fluoride where the ACSE matched the accuracy of the computationally more expensive multireference configuration-interaction method with single and double excitations plus Davidson's Q correction (MRCI+Q).[50]

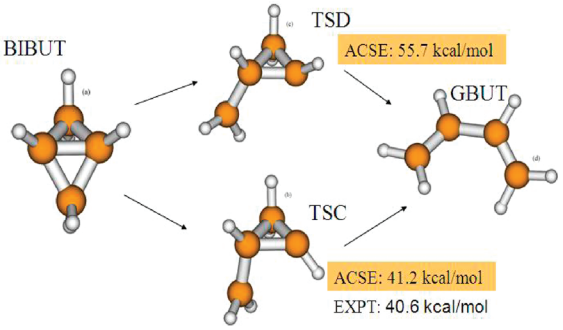

Figure 1. The ring-opening of bicyclobutane to *gauche*-1,3-butadiene can occur by conrotatory or disrotatory pathways where the energy barrier for the disrotatory pathway includes the energy of a strongly correlated biradical transition state. The solution of the ACSE in the 6-311G** basis set predicts 41.2 and 55.7 kcal/mol reaction barriers for the conrotatory and disrotatory pathways, respectively.

Importantly, unlike MRCI+Q, the ACSE is size extensive, that is, it has the correct scaling with system size. Calculations have shown that this property becomes important in only slightly larger molecular systems. Recently, the generalization of the ACSE for excited states and arbitrary spin has been applied to computing (i) the conical intersection in the triplet excited states of methylene[53] and (ii) the photochemical conversion of the allyl radical to the cyclopropyl radical.

The conical intersection between methylene's excited triplet states $1\ ^3A_2$ and $2\ ^3B_1$ is shown in Figure 2. In each plot, the points represent the values computed by full configuration interaction (FCI) in the correlation-consistent polarized valence double-ζ (cc-pVDZ) basis set. The FCI results are compared with those from (a) multireference self-consistent field (MCSCF), (b) second-order multireference perturbation theory (MRPT2), and (c) the ACSE. The ACSE improves the accuracy of MCSCF by 2 orders of magnitude and MRMP2 by 1 order of magnitude. The average differences in the MCSCF, MRMP2, and ACSE energies from FCI are 93.89, 12.27, and 1.51 mhartree, respectively.[53] Similar accuracy was obtained at the conical intersection. The location of the intersection computed by the ACSE corroborates Yarkony's results[114] with a high degree of accuracy. Furthermore, the ACSE produces nearly *N*-representable 2-RDMs from which both one- and two-particle properties can be computed without any additional calculations.

Photoexcited chemical reactions provide a critical pathway for chemical transformation in both nature and materials.[115] The ring closing of allyl radical to cyclopropyl radical and the reverse reaction, the ring opening of cyclopropyl radical, are prototype reactions for *electrocyclic reactions* in organic chemistry. Recently, Foley, Rothman, and the author[55] applied the ACSE method to compute the ground- and excited-state energies and 2-RDMs of reactants, products, and transition states in the interconversion of the allyl and cyclopropyl radicals. Results are shown in Figure 3. We find that the conrotatory and disrotatory reaction barriers from ground-state allyl radical to the cyclopropyl radical are large while these barriers from excited-state allyl radical are negligible, essentially nonexistent. Calculations of the occupation numbers of the natural orbitals reveal strong multireference correlation in the excited states. Comparisons were made with multireference second- and third-order perturbation theories and multireference configuration interaction. While predicted energy differences do not vary greatly between methods, the ACSE appears to improve

dx.doi.org/10.1021/cr2000493 |*Chem. Rev.* 2012, 112, 244–262

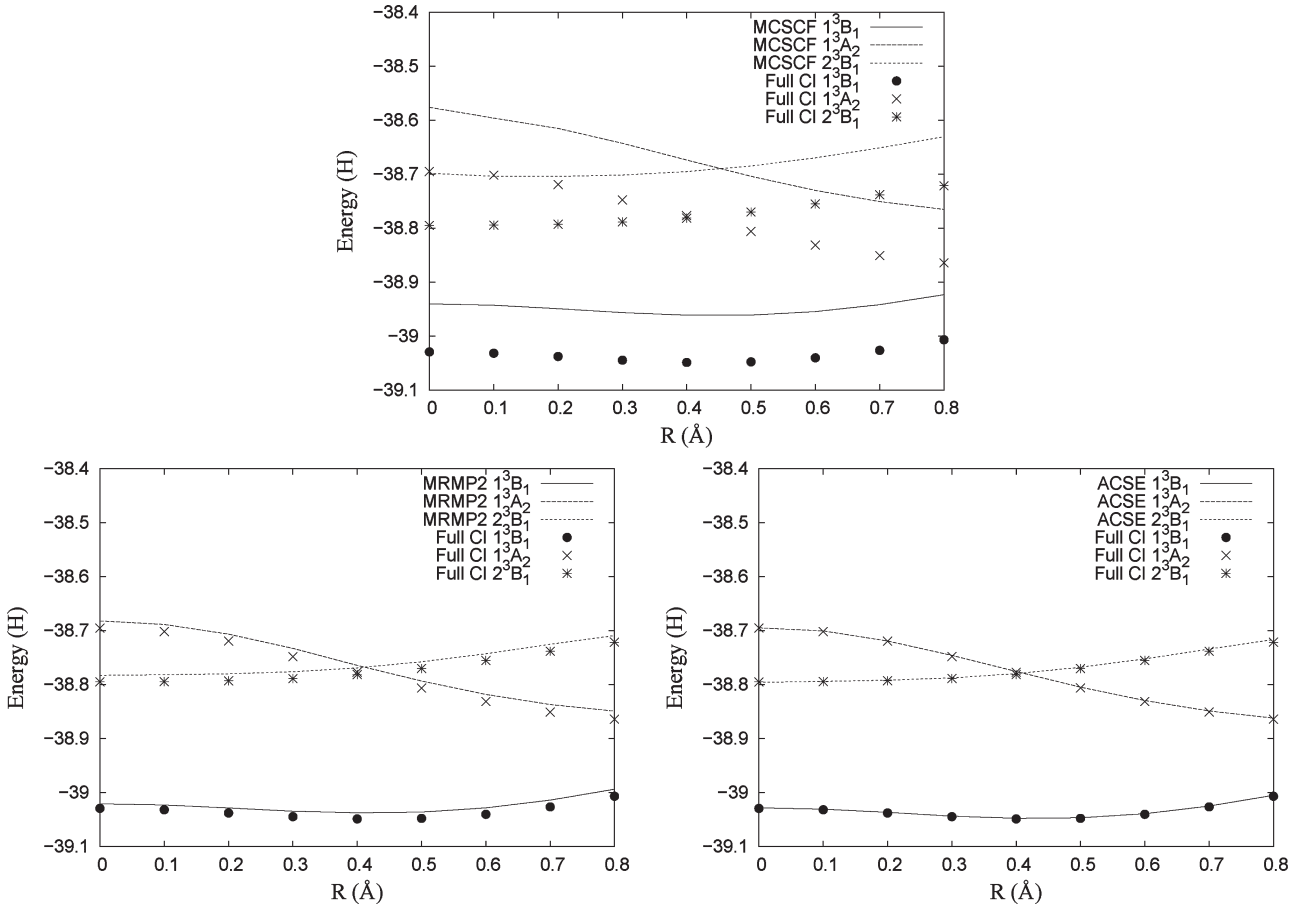

Figure 2. The (a) MCSCF (top), (b) MRMP2 (middle), and (c) ACSE (bottom) potential energy curves for the 1 $^3B_1$, 1 $^3A_2$, and 2 $^3B_1$ states of methylene, as functions of *R*, plotted against those from FCI, given by data points. Reprinted with permission from ref 53. Copyright 2010 American Institute of Physics.

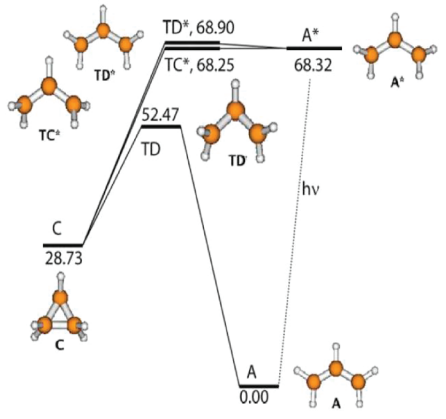

Figure 3. The ring opening of allyl radical (A) to cyclopropyl (C) radical can occur by a disrotatory ground-state pathway or after excitation to excited allyl (A*) radical by either a disrotatory or a conrotatory excited-state pathway. Energy barriers in kcal/mol are determined from solving the ACSE for the 2-RDM in the 6-311G** basis set.

these differences when they involve a strongly and a weakly correlated radical by capturing a greater share of single-reference correlation that increases the stability of the weakly correlated radicals. For example, the ACSE predicts a −39.6 kcal/mol conversion of the excited allyl radical to the ground-state cyclopropyl radical in comparison to the −32.6 to −37.3 kcal/mol conversions predicted by multireference methods.[55]

3. VARIATIONAL 2-RDM METHOD

Although the ground-state energy of any many-electron atom or molecule can be written as a linear functional of the 2-RDM as shown in eq 16, it cannot be variationally optimized as a functional of the 2-RDM without explicit constraints known as *N*-representability conditions to ensure that the 2-RDM represents an *N*-electron quantum system.[7,11,116] While the idea of a variational 2-RDM method for computing the ground-state energy of a many-electron system arose in the 1950s in the work of Coleman,[8] Lowdin,[10] and Mayer,[9] efforts were stymied by the search for suitable *N*-representability conditions, known as the *N*-representability problem.

Progress in the late 1990s on computing the 2-RDM directly from the approximate solution of the CSE,[16,18−22] described in section 2 led to a renewed interest in the variational calculation of the 2-RDM. In 1998, the author[21] studied reconstructing the 3- and 4-RDMs from the 2-RDM in the CSE by restricting them to be positive semidefinite. Shortly thereafter, Erdahl and Jin[117] and Mazziotti and Erdahl[56] explored in the context of spin models restricting all forms of the 3- and 4-RDMs to be positive semidefinite, which they called 3- and 4-positivity conditions. In 2001,

dx.doi.org/10.1021/cr2000493 |*Chem. Rev.* 2012, 112, 244–262

Nakatsuji and his collaborators[57] and Mazziotti[58] implemented the variational 2-RDM method with 2-positivity conditions and some partial 3-positivity conditions for a collection of atoms and molecules. In 2004, Percus and his collaborators[63] implemented partial 3-positivity conditions, T_1 and T_2 conditions,[69,72,118] which had been proposed in 1978 by Erdahl,[118] and Mazziotti[64,65] introduced a much faster optimization algorithm that extended the variational 2-RDM method to larger molecules and basis sets. The full 3-positivity conditions were first implemented in 2006.[73,74]

In section 3.1, we develop the systematic hierarchy of N-representability constraints for the 2-RDM known as the p-positivity conditions.[7] Minimizing the ground-state energy with respect to the 2-RDM constrained by positivity conditions requires a special type of optimization known as semidefinite programming,[56−58,64,65,77,119] which we review in section 3.2. Finally, in section 3.3, we illustrate the variational 2-RDM method with applications to studying strong electron correlation in acene chains, hydrogen lattices, and firefly luciferin.

3.1. Positivity Conditions

General p-particle N-representability conditions on the 2-RDM are derivable from metric (or overlap) matrices. From the ground-state wave function $|\Psi\rangle$ and a set of p-particle operators $\{\hat{C}_{i_1,i_2,\ldots,i_p}\}$, a set of basis functions can be defined

$$\langle\Phi_{i_1,i_2,\ldots,i_p}| = \langle\Psi|\hat{C}_{i_1,i_2,\ldots,i_p} \tag{29}$$

for which the metric (or overlap) matrix M with elements

$$M^{i_1,i_2,\ldots,i_p}_{j_1,j_2,\ldots,j_p} = \langle\Phi_{i_1,i_2,\ldots,i_p}|\Phi_{j_1,j_2,\ldots,j_p}\rangle \tag{30}$$

$$= \langle\Psi|\hat{C}_{i_1,i_2,\ldots,i_p}\hat{C}^{\dagger}_{j_1,j_2,\ldots,j_p}|\Psi\rangle \tag{31}$$

must be positive semidefinite. We indicate that a matrix has this property by the notation $M \geq 0$. For a p-RDM that is parametrized by a wave function, these vector-space restrictions are *always* satisfied. More generally, however, these conditions, known as *p-positivity conditions*,[56,58,64,65,73,74] offer a systematic approach for imposing N-representability conditions on an RDM *without* using the wave function.

3.1.1. 2-Positivity. When $p = 2$, we may choose the $\hat{C}_{i,j}$ in three distinct ways: (i) to create one particle in the jth orbital and one particle in the ith orbital, that is, $\hat{C}_{i,j} = a^{\dagger}_i a^{\dagger}_j$, (ii) to annihilate one particle in the jth orbital and one particle in the ith orbital (or create holes in each of these orbitals), $\hat{C}_{i,j} = a_i a_j$, and (iii) to annihilate one particle in the jth orbital and create one particle in the ith orbital, that is, $\hat{C}_{i,j} = a^{\dagger}_i a_j$. These three choices for the $\hat{C}_{i,j}$ produce the following *three* different metric matrices for the 2-RDM:

$${}^2D^{i,j}_{k,l} = \langle\Psi|a^{\dagger}_i a^{\dagger}_j a_l a_k|\Psi\rangle \tag{32}$$

$${}^2Q^{i,j}_{k,l} = \langle\Psi|a_i a_j a^{\dagger}_l a^{\dagger}_k|\Psi\rangle \tag{33}$$

$${}^2G^{i,j}_{k,l} = \langle\Psi|a^{\dagger}_i a_j a^{\dagger}_l a_k|\Psi\rangle \tag{34}$$

which must be positive semidefinite if the 2-RDM is N-representable.[56,73,116] All three matrices contain equivalent information in the sense that rearranging the creation and annihilation operators produces linear mappings between the elements of the three matrices; particularly, the two-hole RDM, ${}^2Q$, and the particle−hole RDM, ${}^2G$, may be written in terms of the two-particle RDM, ${}^2D$, as follows

$${}^2Q^{i,j}_{k,l} = 2\,{}^2I^{i,j}_{k,l} - 4\,{}^1D^i_k \wedge {}^1I^j_l + {}^2D^{i,j}_{k,l} \tag{35}$$

and

$${}^2G^{i,j}_{k,l} = {}^1I^j_l\,{}^1D^i_k - {}^2D^{i,j}_{k,l} \tag{36}$$

where ${}^1I$ and ${}^2I$ are the one- and two-particle identity matrices and $\wedge$ denotes the Grassmann wedge product.[21] While all three matrices are interconvertible, the nonnegativity of the eigenvalues of one matrix does not imply the nonnegativity of the eigenvalues of the other matrices, and hence, the restrictions ${}^2Q \geq 0$ and ${}^2G \geq 0$ provide two important N-representability conditions in addition to ${}^2D \geq 0$. These conditions physically restrict the probability distributions for two particles, two holes, and one particle and one hole to be nonnegative with respect to all unitary transformations of the one-particle basis set. Collectively, the three restrictions are known as the *2-positivity* conditions.[56,58,64,65,73]

Because ${}^2D \geq 0$ and ${}^2Q \geq 0$ imply ${}^1D \geq 0$ and ${}^1Q \geq 0$ by contraction

$${}^1D^i_k = \frac{1}{N-1}\sum_j {}^2D^{i,j}_{k,j} \tag{37}$$

$${}^1Q^i_k = \frac{1}{r-N-1}\sum_j {}^2Q^{i,j}_{k,j} \tag{38}$$

the 2-positivity conditions imply the 1-positivity conditions. The r in the contraction of the two-hole RDM denotes the rank of the one-particle basis set. In general, the p-positivity conditions imply the q-positivity conditions for $q \leq p$. The 1-positivity conditions from the metric matrices for the one-particle and one-hole RDMs, ${}^1D$ and ${}^1Q$, restrict the occupation numbers n_i (or eigenvalues) of the 1-RDM to lie in the interval $n_i \in [0,1]$. Coleman showed this condition on the eigenvalues to be both *necessary and sufficient* for the N-representability of the 1-RDM.[11]

3.1.2. 3-Positivity. The conditions that a 3-RDM be 3-positive follow from writing the operators in eq 29 as products of *three* second-quantized operators.[56,58,73,117] The resulting basis functions lie in four vector spaces according to the number of creation operators in the product. Basis functions between these vector spaces are orthogonal because they are contained in Hilbert spaces with different numbers of particles. The four metric matrices that must be constrained to be positive semidefinite for 3-positivity[56] are given by

$${}^3D^{i,j,k}_{p,q,r} = \langle\Psi|a^{\dagger}_i a^{\dagger}_j a^{\dagger}_k a_r a_q a_p|\Psi\rangle \tag{39}$$

$${}^3E^{i,j,k}_{p,q,r} = \langle\Psi|a^{\dagger}_i a^{\dagger}_j a_k a^{\dagger}_r a_q a_p|\Psi\rangle \tag{40}$$

$${}^3F^{i,j,k}_{p,q,r} = \langle\Psi|a_i a_j a^{\dagger}_k a_r a^{\dagger}_q a^{\dagger}_p|\Psi\rangle \tag{41}$$

$${}^3Q^{i,j,k}_{p,q,r} = \langle\Psi|a_i a_j a_k a^{\dagger}_r a^{\dagger}_q a^{\dagger}_p|\Psi\rangle \tag{42}$$

Physically, because ${}^3D$ is the metric (or overlap) matrix of basis functions in which three particles have been "killed", the condition that ${}^3D$ be positive semidefinite, ${}^3D \geq 0$, restricts the probability distribution for "three particles" to be nonnegative. Because ${}^3E$ is the metric matrix of basis functions in which two particles and one hole have been "killed", the condition ${}^3E \geq 0$ restricts the probability distribution for "two particles and one hole"

to be nonnegative. Similarly, the conditions ${}^3F \geq 0$ and ${}^3Q \geq 0$ restrict the probability distributions for "one particle and two holes" and "three holes" to be nonnegative.

As in eqs 35 and 36 for the 2-positive metric matrices, the 3-positive metric matrices are connected by linear mappings, which can be derived by rearranging the second-quantized operators. For example, the mapping from ${}^3D$ to ${}^3Q$ may be written with the Grassmann wedge product[21,120] as

$$ {}^3Q^{i,j,k}_{p,q,r} = 6\,{}^3I^{i,j,k}_{p,q,r} - 18\,{}^1D^{i}_{p} \wedge {}^2I^{j,k}_{q,r} + 9\,{}^2D^{i,j}_{p,q} \wedge {}^1I^{k}_{r} - {}^3D^{i,j,k}_{p,q,r} \quad (43) $$

where ${}^1I$, ${}^2I$, and ${}^3I$ are the one-, two-, and three-particle identity matrices. Similar mappings can be derived to express ${}^3E$ and ${}^3F$ as functionals of ${}^3D$. Contraction of the 3-positivity matrices in eq 39 generates the 1- and 2-positivity metric matrices, and hence, the 3-positivity conditions imply the 1- and 2-positivity conditions. A 2-RDM is defined to be 3-positive if it arises from the *contraction* of a 3-positive 3-RDM:

$$ {}^2D^{i,j}_{p,q} = \frac{1}{N-2}\sum_k {}^3D^{i,j,k}_{p,q,k} \quad (44) $$

The 3-positivity conditions have been examined in variational 2-RDM calculations on spin[56,56,117,121] and molecular[73,74] systems where they give highly accurate energies and 2-RDMs.

3.2. Semidefinite Programming

Variational calculation of the energy with respect to the 2-RDM constrained by 2-positivity conditions requires minimizing the energy in eq 16 while restricting the ${}^2D$, ${}^2Q$, and ${}^2G$ to be not only positive semidefinite but also interrelated by the linear mappings in eqs 35−38. This is a special optimization problem known as a *semidefinite program*. The solution of a semidefinite program is known as *semidefinite programming*.[77,119,122,123]

In the mid-1990s, a powerful family of algorithms, known as *primal-dual interior-point algorithms*, was developed for solving semidefinite programs.[119] The phrase *interior-point* means that the method keeps the trial primal and dual solutions on the *interior* of the feasible set throughout the solution process. In these algorithms, a good initial guess for the 2-RDM is a scalar multiple of the two-particle identity matrix. Advantages of the interior-point methods are (i) rapid quadratic convergence from the identity matrix to the optimal 2-RDM for a set of positivity conditions and (ii) a rigorous criterion in the duality gap for convergence to the global minimum. These benefits, however, are accompanied by large memory requirements and a significant number of floating-point operations per iteration, specifically $O(nm^3 + n^2m^2)$ where n is the number of variables and m is the number of constraints. With m and n proportional to the number of elements in the 2-RDM ($\sim r^4$), the method scales approximately as r^{16} where r is the rank of the one-particle basis set.[58,60] The variational 2-RDM method has been explored for minimal basis sets with the primal-dual interior-point algorithm, but the computational scaling significantly limits both the number of active electrons and the size of the basis set.[57−60,62,63]

The author developed a large-scale semidefinite programming algorithm for solving the semidefinite program in the variational 2-RDM method.[64,65,73,77] The optimization challenge in the 2-RDM method is to constrain the metric matrices to be positive semidefinite while the ground-state energy is minimized. The algorithm constrains the solution matrix M to be positive semidefinite by a matrix factorization

$$ M = RR^* \quad (45) $$

where for the 2-positivity conditions M contains the ${}^2D$, ${}^2Q$, and ${}^2G$ matrices. Such a matrix factorization had been previously considered in the context of 2-RDM theory by Rosina,[124] Harriman,[125] and the author,[21] and it had been employed for solving large-scale semidefinite programs in combinatorial optimization.[126] The applications in Mazziotti[64,65] and Burer and Choi[127] were the first to apply the matrix factorization to semidefinite programs with multiple diagonal blocks in the solution matrix M. The linear constraints, including the trace, the contraction, and the interrelations between the metric matrices, become quadratic in the new independent variables R. Therefore, the factorization in eq 45 converts the semidefinite program into a *nonlinear program* where the energy must be minimized with respect to R while nonlinear constraint equalities are enforced.

We can solve the nonlinear formulation of the semidefinite program by the augmented Lagrange multiplier method for constrained nonlinear optimization.[64,65,77,126,128] Consider the augmented Lagrangian function

$$ L(R) = E(R) - \sum_i \lambda_i c_i(R) + \frac{1}{\mu}\sum_i c_i(R)^2 \quad (46) $$

where R is the matrix factor for the solution matrix M, $E(R)$ is the ground-state energy as a function of R, $\{c_i(R)\}$ is the set of equality constraints, $\{\lambda_i\}$ is the set of Lagrange multipliers, and μ is the penalty parameter. For an appropriate set of multipliers $\{\lambda_i\}$, the minimum of the Lagrangian function with respect to R corresponds to the minimum of the energy $E(R)$ subject to the nonlinear constraints $c_i(R)$. The positive third term in the augmented Lagrangian function, known as the quadratic penalty function, tends to zero as the constraints are satisfied.

The cost of the algorithm is dominated by r^6 floating-point operations,[64] mainly from the matrix multiplication of the block-diagonal R matrix with itself, where r is the rank of the one-particle basis set. Storage of the factorized 2-RDM, several copies of its gradient, and the Lagrange multipliers scales as r^4. In comparison with the primal-dual interior-point approach, which scales as r^{16} and r^8 in floating-point operations and memory storage, the first-order nonlinear algorithm for the variational 2-RDM method[64,65,77] provides a significant improvement in computational efficiency. The efficiency of the matrix factorization has been confirmed by Cancés, Stoltz, and Lewin,[129] who studied a dual formulation of the problem. Verstichel et al.[130] have introduced a first-order interior-point algorithm, and recently, the author[131] has developed a boundary-point algorithm that is shown to be at least 10−20 times faster than the efficient matrix-factorization algorithms.

3.3. Applications

Because the N-representability conditions are independent of a reference wave function, the variational 2-RDM method can capture strong electron correlation effects in molecules. To illustrate this ability, we discuss previous applications of the variational 2-RDM method to (i) the dissociation of the N_2 molecule,[73] (ii) the prediction of the metal-to-insulator transition in the H_{64} lattice,[81] and (iii) the emergence of polyradical character in acene chains.[78]

3.3.1. Dissociation of the N_2 Molecule. The ground-state energy of the nitrogen molecule as a function of bond length is examined with 2-RDM and wave function methods, coupled

dx.doi.org/10.1021/cr2000493 |Chem. Rev. 2012, 112, 244–262

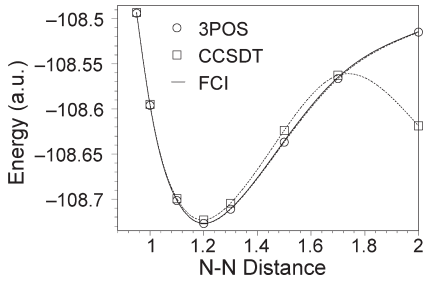

Figure 4. Comparison of the 3POS and CCSDT potential energy curves denoted by dashed lines with the FCI curve denoted by a solid line. The variational lower-bound 3POS curve is essentially indistinguishable from the FCI curve. Reprinted with permission from ref 73. Copyright 2006 American Physical Society.

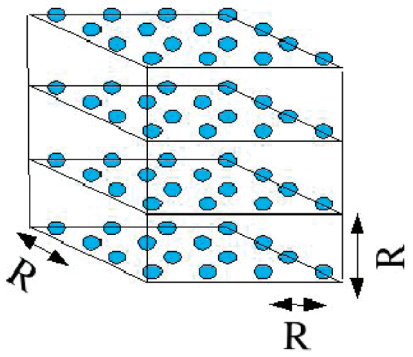

Figure 5. Sketch of the 4 × 4 × 4 hydrogen cube. Reprinted with permission from ref 81. Copyright 2010 American Institute of Physics.

cluster with single, double, and triple excitations (CCSDT) and full configuration interaction (FCI), in Figure 4.[73] Minimal Slater-type orbital basis sets (STO-6G) are employed, and all valence electrons are correlated. The variational lower-bound 3POS curve is essentially indistinguishable from the FCI curve. The 2-RDM method with 3-positivity (3POS) has a maximum error of −1.4 mhartree at R = 1.7 Å. The 2-positivity (2POS) and 2-positivity plus $T_1\overline{T}_2$ conditions yield maximum errors of −23.6 and −4.6 mhartree at R = 1.7 Å. Around equilibrium, the 3-positivity improves the energies from 2-positivity plus $T_1\overline{T}_2$ and 2-positivity by 1 and 2 orders of magnitude, respectively, and it is an order of magnitude more accurate than CCSDT.

3.3.2. Metal-to-Insulator Transition in the H_{64} Lattice. For the 4 × 4 × 4 cube (Figure 5), RHF and MP2 provide incorrect dissociation limits, and the coupled-cluster calculations diverge for nonequilibrium interatomic distances $R \geq 1.5$ Å. In contrast, as shown in Figure 6, the 2-RDM method with 2-positivity conditions ensures that upon dissociation the cluster energies per atom converge to the energy of an isolated H atom in the given basis set.[81] Importantly, the dissociation of the 4 × 4 × 4 cube would require approximately 10^{18} equally weighted determinants in a conventional wave function calculation, which is a *billion times more determinants* than are treatable with a standard multireference self-consistent-field calculation.

The metal-to-insulator transition for the 4 × 4 × 4 cube is shown in Figure 7.[81] In the variational 2-RDM method, the magnitude of the off-diagonal 1-RDM elements in the atomic-orbital basis set, measured by harmonic average γ, decays as the interatomic distance R increases, while in the RHF method, the

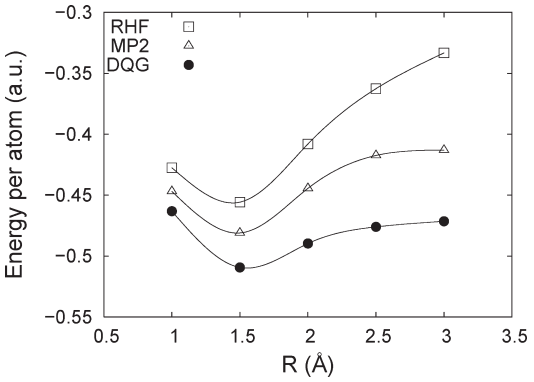

Figure 6. Potential energy curve for the symmetric dissociation of the 4 × 4 × 4 hydrogen cube, reported per atom, as a function of the distance between the closest atoms. Reprinted with permission from ref 81. Copyright 2010 American Institute of Physics.

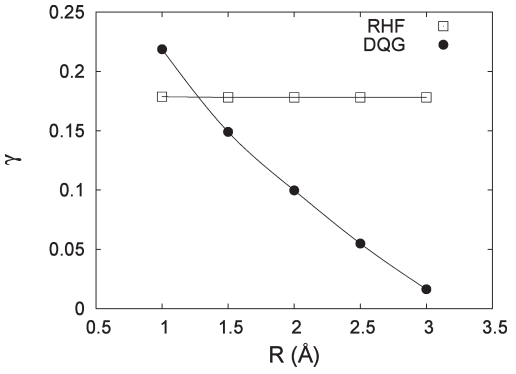

Figure 7. Metal-to-insulator transition in the 4 × 4 × 4 hydrogen cube under the change of the distance R between closest atoms. Reprinted with permission from ref 81. Copyright 2010 American Institute of Physics.

harmonic average γ rapidly converges to a positive limit. Note that the aggregate measure γ decreases more gradually than the measure ${}^1D_{1n}$ for two hydrogen atoms at diagonal vertices.

3.3.3. Polyradical Character of the Acene Chains. The active spaces necessary to describe the π electrons in the n-acene series where n = 2−8 (see Figure 8) become prohibitively large for n > 4 because the dimension of the CI Hamiltonian scales exponentially with the number of electrons. For example, even a calculation of tetracene (4-acene) would require computing the lowest eigenvector of a Hamiltonian with dimension ∼1.12 × 10^8, which already presents a formidable challenge in terms of both storage and time for traditional CASSCF approaches. While a CASSCF study of octacene would demand the diagonalization of a Hamiltonian of dimension ∼1.47 × 10^{17}, the approximate ground-state energy and 2-RDM can be readily computed within the framework of the variational 2-RDM method with two-positivity conditions.

In ref 78, we studied the change in the natural-orbital occupation numbers with both chain length and basis-set size. Half of the available π orbitals of the double-ζ basis set were included in the active space. Figure 9 shows the natural-orbital occupation numbers for acenes with chain lengths n ranging from two to eight. The onset of biradical character is evident because the

dx.doi.org/10.1021/cr2000493 |*Chem. Rev.* 2012, 112, 244–262

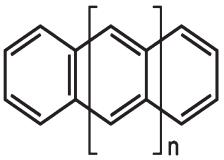

Figure 8. Sketch of general acene chains of length *n*.

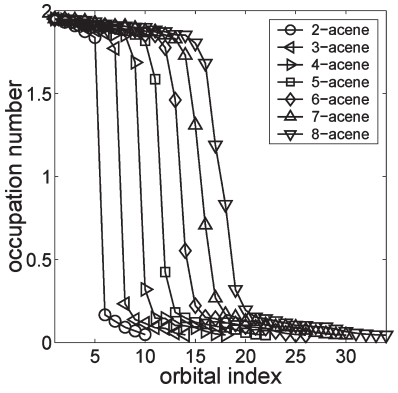

Figure 9. Natural orbital occupation numbers for the *n*-acene series ($n = 2-8$). The basis set is double-ζ, and calculations are performed with an active space that includes the $4n + 2$ lowest lying π molecular orbitals. Reprinted with permission from ref 78. Copyright 2008 American Institute of Physics.

difference between the occupation numbers of the highest-occupied and lowest-unoccupied natural orbitals decreases with increasing chain length. The difference is as large as 1.67 for napthalene and as small as 0.36 for octacene. Furthermore, around $n = 8$, we begin to observe the emergence of polyradical character in the chains. While the increase in basis set from STO-3G to double-ζ substantially decreases the energy, it does not significantly change either the occupation numbers or the trends in radical character.

3.3.4. Conical Intersections in Dioxetanone and Firefly Luciferin. Dioxetanone is a key moiety of the luciferin molecule whose reactions in the firefly are responsible for its bioluminescence (Figures 10). Recent calculations of firefly luciferin employed four active electrons in four active orbitals to describe the strong electron correlation in the dioxetanone moiety,[132] but Liu et al. showed that the decomposition reaction for dioxetanone with two conical intersections on its potential energy surface[133] requires an active space that is significantly larger than (4,4) to capture the electron correlation.[133] How many *active orbitals* are needed to describe the strong electron correlation in the luminescence reactions of dioxatenone and firefly luciferin?

Recently, Greenman and the author[100] applied the variational 2-RDM method with 2-positivity conditions to studying the convergence of the ground-state potential energy surface of dioxetanone with active-space size. Calculations treated active spaces ranging from (4,4) through (20,17). Because the 2-RDM method *scales polynomially with system size*, it can treat large (18,15) and (20,17) active spaces of dioxetanone that would be very difficult or impossible to study with conventional CASSCF methods. We measured the strong electron correlation along the reaction coordinate with two RDM-based metrics, the von Neumann entropy of the 1-RDM and the Frobenius norm

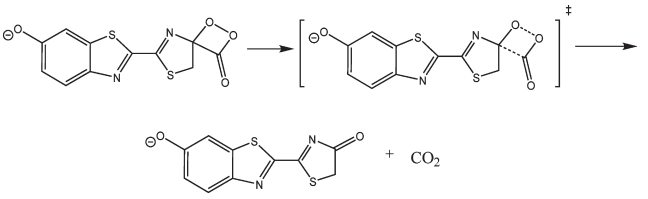

Figure 10. The chemiluminescent portion of the firefly luciferin reaction is shown. First, firefly luciferin begins to decompose to oxyluciferin and carbon dioxide. The excited state of the oxyluciferin can be accessed through a conical intersection, and eventually light is emitted to reach ground-state oxyluciferin. Reprinted with permission from ref 100. Copyright 2010 American Institute of Physics.

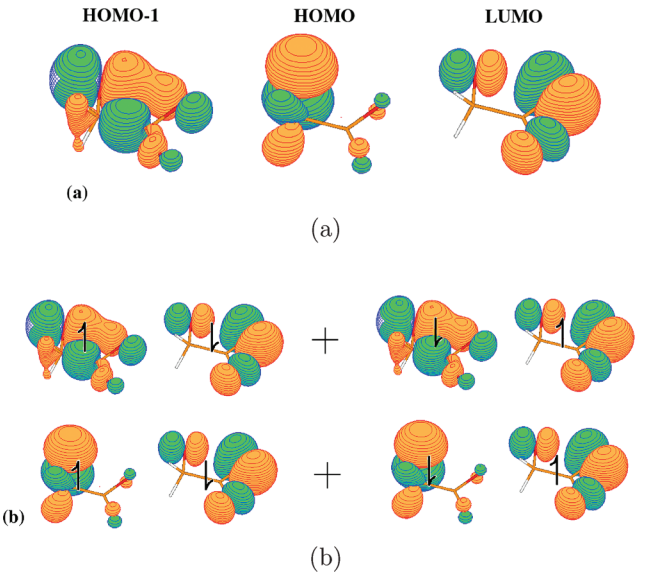

Figure 11. An analysis of the elements comprising the infinity norm of the cumulant 2-RDM showed that the smaller active spaces substantially overcorrelate the two-electron configurations (Lα,Hβ) and (Hα,Lβ) while undercorrelating the configurations (Lα,(H $-$ 1)β) and ((H $-$ 1)α,Lβ) where H and L denote the HOMO and LUMO orbitals. The H $-$ 1, H, and L orbitals are shown in panel a, while the pair of entangled two-electron configurations (Lα,Hβ) + (Hα,Lβ) and (Lα,(H $-$ 1)β) + ((H $-$ 1)α,Lβ) are displayed in panel b. Reprinted with permission from ref 100. Copyright 2010 American Institute of Physics.

(or infinity norm) of the cumulant 2-RDM.[134−136] At a point near the first conical intersection *both the von Neumann entropy and the infinity norm showed clearly that the correlation effects are not converged until at least the (14,12) active space*. An analysis of the elements comprising the infinity norm of the cumulant 2-RDM showed that the smaller active spaces substantially overcorrelate the two-electron configurations (Lα,Hβ) and (Hα,Lβ) while undercorrelating the configurations (Lα,(H $-$ 1)β) and ((H $-$ 1)α,Lβ) where H and L denote the HOMO and LUMO orbitals (Figure 11).

From the calculations with dioxetanone *Greenman and the author predicted that firefly luciferin will require an active space of 28 electrons in 25 orbitals*,[100] which significantly exceeds recent (12,12) MCSCF calculations.[132] The dioxetanone calculations, in conjunction with previous calculations on acene and aryne chains,[78,80] show that the variational 2-RDM method offers a viable approach to studying strong electron correlation in large

dx.doi.org/10.1021/cr2000493 |*Chem. Rev.* 2012, 112, 244–262

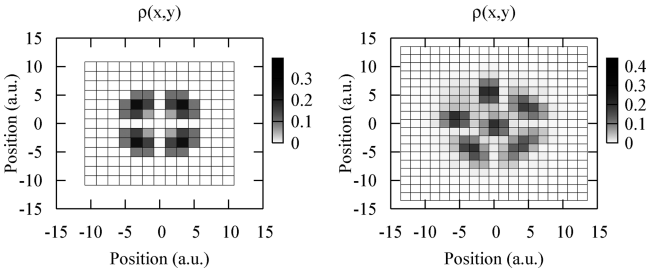

Figure 12. Densities of four and six helium atoms in two dimensions. Reprinted with permission from ref 38. Copyright 2007 American Physical Society.

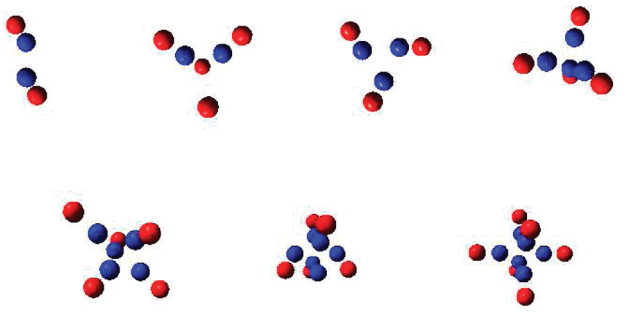

Figure 13. Global minimum of binary Morse clusters located by the 2-particle reduced density matrix function with semidefinite programming. The blue atoms are of type A, and the red atoms are of type B. Reprinted with permission from ref 103. Copyright 2008 American Physical Society.

active spaces of molecular systems where traditional CASSCF calculations are prohibited by cost.

3.3.5. Ground-State Nuclear Motion. The direct variational calculation of the two-particle reduced density matrix has also been extended to study the ground-state motion of nuclei. Here we briefly summarize three areas in which the 2-RDM method has been applied to nuclear motion: (i) the probability distributions of nuclei within the Born−Oppenheimer approximation,[38] (ii) the global minima of nuclei within the classical limit,[103] and (iii) the probability distributions of *nuclei and electrons* beyond the Born−Oppenheimer approximation.[79]

Kamarchik and the author[38] developed a few-particle variational RDM theory for treating ground-state nuclear motion in atomic and molecular clusters and potentially molecules. Two features of the RDM method for nuclear motion that differ from the electronic theory are the derivation and application of generalized *N*-representability conditions for (i) *multiple* types of particles and (ii) *three- or higher-body* interactions. Preliminary applications were made to clusters of noble gases and small molecules such as acetylene. In Figure 12, the ground-state one-particle probability distribution is shown for He_4 and He_6 clusters.[38] The probability distributions of the nuclei were computed by solving a semidefinite program with the program RRSDP.[64] The quantum mechanical blueprints reveal a "blurring" of the classical square and pentagonal structures. By adjusting the mass of the particles, we can tune the clusters anywhere between classical structures and Bose condensates. *For the first time by looking at just two helium atoms, we obtain the quantum vibrational structure of all four or six helium atoms.* Unlike mean field theory, the RDM method is a fully correlated theory where the *N*-representability conditions allow the RDM to represent a correlated *N*-particle wave function. Integration of the 2-RDM yields the one-density, which furnishes an intuitive blueprint showing the most probable positions of all *N* nuclei and the extent of the ground-state quantum motion.

In molecular science, a significant problem is the computation of a molecule's (or molecular cluster's) configuration that globally minimizes its energy. Calculating the global energy minimum, however, is especially challenging for two reasons: (i) the exponential dependence of the problem on the number *N* of particles, and (ii) the large number of local minima that must be distinguished from the global minimum. Kamarchik and the author[103] developed a polynomial-time algorithm for computing the global minima of classical molecular clusters with pairwise interactions as a function of only the two-particle reduced density function, which expresses the probability for finding two particles in the field of the other particles. Taking the classical limit of the 2-RDM method for nuclear probability distributions in clusters produces a new formulation of the global optimization problem for classical systems of particles, where combinatorial optimization over *N* indistinguishable particles is replaced by a convex optimization over just two particles. Importantly, while the conventional combinatorial problem scales as *r* choose *N* where *r* is the number of lattice points (a nonpolynomial (NP) scaling known as NP hard), the convex reformulation can be relaxed to scale as *r* choose 2 (a polynomial-time scaling).

An essential ingredient of the global-energy-minimum method is a new set of classical *N*-representability conditions that were derived in ref 103 from the classical limit of the quantum *N*-representability conditions. Like their quantum counterparts, the classical *N*-representability conditions can be formulated as semidefinite constraints on matrices, and hence, the optimization can be formulated as a semidefinite program that is solvable by the RRSDP program. Application of the method to clusters of 4−12 alkali atoms reproduced the exact global minima generated by a stochastic sampling algorithm of Wales.[137] As in the quantum limit, more than one type of atom can also be treated. Figure 13 shows an application of the method to computing the global minima of binary atomic clusters where the atoms interact pairwise by Morse potentials.[103] The different structures arise from varying the number of type A (blue) and type B (red) alkali atoms. Because there exists a mapping between the global optimization problem of molecular clusters and the cut-polytope problems in combinatorial optimization, this work has potential applications to many other areas of scientific study including the max-cut problem in circuit design and spin glasses, lattice holes in the geometry of numbers, the generalization of density functional theory from the one density to the pair density, and the investigation of generalized Bell's inequalities.

Lastly, Kamarchik and the author[79] extended the variational 2-RDM method for electronic systems to compute ground-state distributions of electrons and hydrogen nuclei in molecules beyond the Born−Oppenheimer approximation. While traditional methods for nuclei rely on the construction of expensive potential energy surfaces or other approximations, the variational 2-RDM method has the advantage of treating both electrons and hydrogen nuclei as quantum-mechanical particles simultaneously. Because these particles interact by pairwise Coulombic potentials, the ground-state energy is expressible as a linear functional of *three* 2-RDMs corresponding to two electrons, two hydrogens, and one electron and one hydrogen. Because the hydrogen atoms

dx.doi.org/10.1021/cr2000493 |*Chem. Rev.* 2012, 112, 244–262

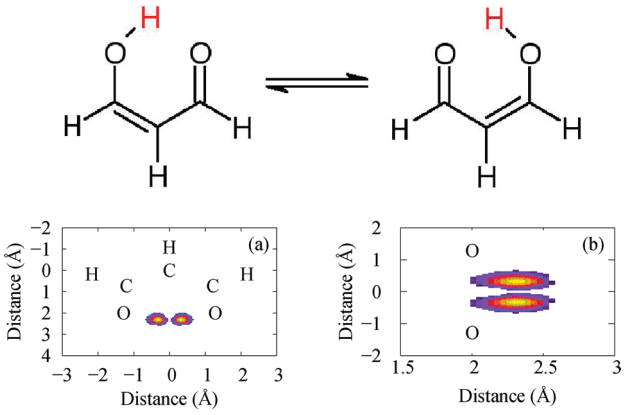

Figure 14. The ground-state nuclear density for the intramolecular hydrogen transfer in malonaldehyde (a) and a close up of the region of interest (b). Each contour line corresponds to a factor of 10 in the density, with the innermost line being 10^{-1}. Reprinted with permission from ref 79. Copyright 2009 American Physical Society.

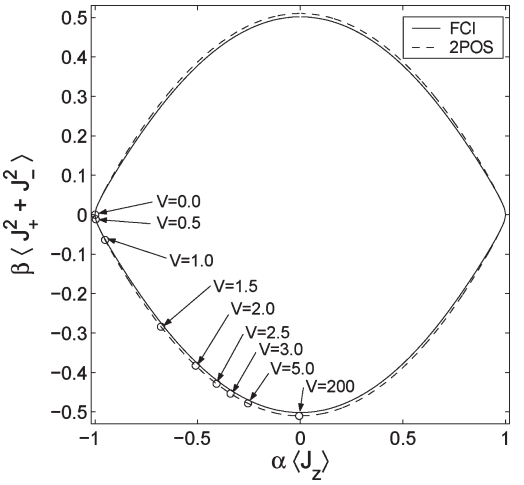

Figure 15. The convex set of 2-positive 2-RDMs (2POS) is compared with the convex set of *N*-representable 2-RDMs (FCI) for the Lipkin model. The 2-positive set contains the *N*-representable set. The circles show the movement of the 2-RDM along the boundary of the set of 2-positive 2-RDMs as a function of the interaction *V*. The significant increase in the "speed" of the 2-RDM around the critical point is a signature of the quantum phase transition. Reprinted with permission from ref 72. Copyright 2006 American Physical Society.

are considerably lighter than the other atoms in most molecules, we treat, as in the work by Hammes-Schiffer,[138] only the hydrogen atoms and the electrons beyond the Born−Oppenheimer approximation. Variational optimization of the ground-state energy requires that the 2-RDMs be restricted by *N*-representability conditions to represent a realistic *N*-particle system where *N* is the total number of electrons and hydrogens. Recent progress in electronic systems with (i) developing necessary *N*-representability conditions and (ii) optimizing the ground-state energy subject to these conditions is extended to systems with two types of particles, electrons and nuclei. The nuclear-electronic 2-RDM method can be applied to studying macroscopic quantum phenomena in molecules with "floppy" or resonant hydrogens. Illustrative applications were made to (i) large-scale hydrogen motion in hydrogen-bonded molecules and protonated acetylene $C_2H_3^+$ and (ii) hydrogen resonance in malonaldehyde $C_3H_4O_2$ and ammonia NH_3. Recently, Chakraborty and Hammes-Schiffer have also cast their nuclear−electron orbital method[138] in a RDM framework.[139]

As an example of using the 2-RDM method to treat both electrons and hydrogen nuclei beyond the Born−Oppenheimer approximation, consider malonaldehyde $C_2H_4O_2$, a simple molecule exhibiting a hydrogen atom resonant between two sites. The ground state of malonaldehyde is typically characterized within the Born−Oppenheimer approximation as one of two asymmetric planar forms (having C_s symmetry),[140] and the Lewis dot structure in Figure 14 shows these two possible structures. In reality, however, the true quantum-mechanical ground state is an equal superposition (or resonance) of these two energetically equivalent configurations. Using the nuclear−electronic 2-RDM method, Kamarchik and the author[79] computed the ground-state nuclear probability density for the hydrogen atom, shown in Figure 14. The 2-RDM computation predicts that the hydrogen atom is resonant (or entangled) between the two sites with equal probability of being at either site. Hence, the ground state of malonaldehyde is a superposition of the two indistinguishable tautomers with C_{2v} symmetry, which is consistent with prior calculations on malonaldehyde.[141]

3.3.6. Quantum Phase Transitions. Quantum mechanical systems can undergo significant changes in properties with a small change in a system parameter such as the doping ratio of a superconductor. These dramatic changes, known as *quantum phase transitions*, are signatures of the quantum world, and the value of the parameter at which the change occurs is called the critical point.[142] In wave mechanics, the transformation at the critical point is associated with either an actual or an avoided level crossing of the energies from ground- and excited-state wave functions where one or more properties, described as *order parameters*, exhibit an abrupt change. In 2006, Gidofalvi and the author[72] developed a different, 2-RDM-based approach to computing and identifying quantum phase transitions,[72,102] which has been applied to investigating quantum phase transitions in Lipkin[72,143] and Ising[102,144] spin models. Verstraete and Cirac[145] have also considered the connection between quantum phase transitions and 2-RDMs.

At the critical point of a quantum phase transition one or more of these expectation values displays dramatic changes. In the language of convex sets, a change in a Hamiltonian parameter across a critical point corresponds to a dramatic movement of the ground-state 2-RDM along the boundary of the convex set where the initial and final points on the boundary of the set are distinguished by significant changes in each of the order parameters. In a second-order phase transition from an avoided level crossing, the ground-state 2-RDM for all values of the critical Hamiltonian parameter is a unique extreme point on the boundary of the set. The signature of a second-order quantum phase transition is *rapid movement of the 2-RDM as a function of the critical Hamiltonian parameter along the boundary of the set.*[72,102]

For a Lipkin model with 50 fermions, the convex sets of *N*-representable 2-RDMs (solid line) and 2-positive 2-RDMs (dotted lines) are shown in Figure 15. The boundaries of the 2-positive and *N*-representable sets are computed by evaluating the expectation values $\langle \hat{J}_z \rangle$ and $\langle \hat{J}_+^{\,2} + \hat{J}_-^{\,2} \rangle$ with respect to the 2-positive and *N*-representable ground-state 2-RDMs of the

dx.doi.org/10.1021/cr2000493 |*Chem. Rev.* 2012, 112, 244–262

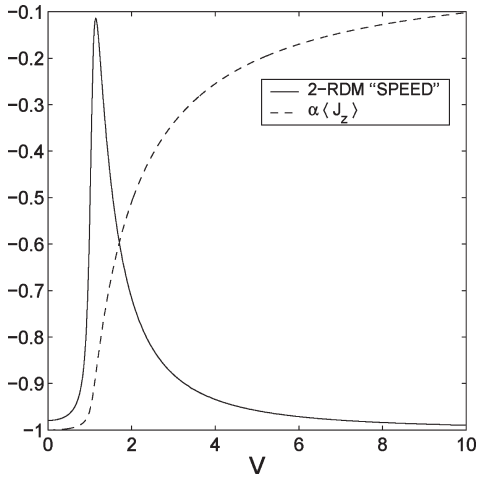

Figure 16. Both the order parameter, $\alpha\langle \hat{J}_z \rangle$, and the "speed" of the 2-RDM, measuring the movement of the 2-RDM on the boundary of the convex set of 2-positive 2-RDMs, show significant changes around the critical point $V \approx 1$ of the phase transition. Reprinted with permission from ref 72. Copyright 2006 American Physical Society.

Lipkin Hamiltonians in ref 72 with $\epsilon = 1$ and $V \in [-200,200]$. Pairs of expectation values $\langle \hat{J}_z \rangle$ and $\langle \hat{J}_+^2 + \hat{J}_-^2 \rangle$ can be obtained from an N-representable 2-RDM if and only if they lie inside the solid curve. Similarly, pairs of expectation values can be obtained from a 2-positive 2-RDM if and only if they lie inside the dashed curve. Because the 2-positivity conditions are necessary but not sufficient N-representability conditions, the convex set of 2-positive 2-RDMs contains the set of N-representable 2-RDMs. Plotting the convex set of 3-positive 2-RDMs in Figure 15 would yield a curve indistinguishable from the N-representable curve.

In the thermodynamic limit, a quantum phase transition occurs in the Lipkin model around $V = 1$. Circles on the dashed curve for the 2-positive set in Figure 15 denote the position of the 2-RDM as a function of the parameter V in the Lipkin Hamiltonian. Between $V = 0$ and $V = 1.0$, the position of the 2-RDM on the boundary of the convex set does not change significantly, but from $V = 1.0$ to $V = 1.5$, where there is a second-order quantum phase transition, the 2-RDM markedly alters its position on the boundary of the set. After the point $V = 1.5$, the derivative in the 2-RDM's position with V decreases. Between $V = 5$ and $V = 200$ the position of the 2-RDM changes less than between $V = 1.0$ and $V = 1.5$. In general, the movement of the 2-RDM in the convex set collectively represents the changes in all of the order parameters.

Figure 16 shows the order parameter $\alpha\langle \hat{J}_z \rangle$ and the "speed" of the 2-RDM defined as $(\vec{v} \cdot \vec{v})^{1/2}$ where $\vec{v} = (\partial\langle \hat{J}_z \rangle/\partial V, \partial\langle \hat{J}_+^2 + \hat{J}_-^2 \rangle/\partial V)$. The *peak* in the 2-RDM "speed" defines the location of the critical point. For the Lipkin model with 50 fermions, the maximum speed occurs at $V = 1.14$. As $N \rightarrow \infty$, calculations show, the peak approaches the location of the critical point in the thermodynamic limit for the model. In the $N \rightarrow \infty$ limit, the derivative of the 2-RDM "speed" becomes discontinuous, which is consistent with a second-order phase transition. Although Gidofalvi and the author[72] illustrate RDM mechanics for quantum phase transitions with the Lipkin model, the concept of 2-RDM "speed" is generally applicable to quantum systems with an arbitrary number of degrees of freedom. For a 2-RDM with n degrees of freedom, the velocity vector generalizes to an n-component vector where each component is the derivative of a degree of freedom with respect to a Hamiltonian parameter like V. Ising[102] and Hubbard[70] models have also been treated.

4. PARAMETRIC 2-RDM METHOD

Both the variational 2-RDM method in section 3 and the contracted Schrödinger methods in section 2 have the ability to capture strong electron correlation that is especially difficult for traditional wave function methods. However, it would also be useful to have a 2-RDM-based method that is designed for treating moderate electron correlation with a combination of speed and accuracy that exceeds that of conventional wave function-based methods. In this section, we develop a parametric variational 2-RDM method[83−91] in which the calculations can be performed at the speed of configuration interaction with single and double excitations (CISD) with an accuracy approaching that of the more expensive coupled cluster methods (CCSDT) where single, double, and triple excitations are included. Although we could derive the family of parametric 2-RDM methods starting from a model wave function,[83] we derive them here from contractions of the cumulant reconstructions in section 2,[91] which provides a rigorously size extensive theory based on the properties of cumulant RDMs. Piris and his co-workers[146,147] have introduced an approach to natural-orbital functional theory that can also be viewed as a type of parametric 2-RDM method.

4.1. Parametrization of the 2-RDM

The 2-RDM can be expressed in terms of the one-particle reduced density matrix (1-RDM or ${}^1D$) and a connected part that cannot be expressed as a Grassmann (wedge) product of the 1-RDM, known as the cumulant (or connected) 2-RDM[7,22−26,28,110,148]

$$ {}^2D_{st}^{pq} = 2\,{}^1D_p^s \wedge {}^1D_t^q + {}^2\Delta_{st}^{pq} \tag{47} $$

Like the 2-RDM, the 1-RDM can be divided into a diagonal mean-field matrix and a correlated matrix that connects multiple determinants

$$ {}^1D_q^p = ({}^1D_o)_q^p + {}^1\Delta_q^p \tag{48} $$

Furthermore, both of the correlated parts of the 1- and 2-RDMs can be decomposed into two *Hermitian* matrices

$$ {}^2\Delta = {}^2T + {}^2R \tag{49} $$

$$ {}^1\Delta = {}^1T + {}^1R \tag{50} $$

where ${}^2T$ is the first-order part of ${}^2\Delta$, ${}^1T$ is the second-order part of ${}^1\Delta$ (the first-order part of ${}^1\Delta$ vanishes), and ${}^2R$ and ${}^1R$ contain higher-order corrections within a renormalized perturbation theory. We can derive part of the ${}^2R$ and ${}^1R$ remainder matrices in terms of the ${}^2T$ and ${}^1T$.[91] Because the single excitation coefficients (${}^1T$) can be made zero by performing orbital rotations to obtain Brueckner-like orbitals,[149] we begin by considering only the ${}^2T$ matrices.

As shown in ref 91, using the *cumulant expansions* for the 3- and 4-RDMs[7,22−26,110,148] in section 2 and their *contraction relations*,[7,28] we can obtain the following parametrizations of the cumulant (connected) parts of the 2-RDMs:

$$ {}^2\Delta_{kl}^{ij} = + \sum_{a<b} {}^2T_{ij}^{ab}\,{}^2T_{kl}^{ab} + O(\lambda^4) \tag{51} $$

dx.doi.org/10.1021/cr2000493 |Chem. Rev. 2012, 112, 244–262

$$ {}^2\Delta^{ia}_{jb} = -\sum_{kc} {}^2T^{ac}_{jk}\,{}^2T^{bc}_{ik} + O(\lambda^4) \quad (52) $$

$$ {}^2\Delta^{ab}_{cd} = +\sum_{i<j} {}^2T^{ab}_{ij}\,{}^2T^{cd}_{ij} + O(\lambda^4) \quad (53) $$

$$ {}^2\Delta^{ab}_{ij} = +{}^2T^{ab}_{ij} + O(\lambda^3) \quad (54) $$

and the connected part of the 1-RDM:

$$ {}^1\Delta^{i}_{j} = -\sum_{k,a<b} {}^2T^{ab}_{ik}\,{}^2T^{ab}_{jk} + O(\lambda^4) \quad (55) $$

$$ {}^1\Delta^{a}_{b} = +\sum_{c,i<j} {}^2T^{ij}_{ac}\,{}^2T^{bc}_{ij} + O(\lambda^4) \quad (56) $$

where $\{i,j,k,l\}$ and $\{a,b,c,d\}$ are the indices for the occupied and virtual orbitals, respectively. These definitions of the 2-RDM elements involve only connected quantities and therefore yield a size extensive 2-RDM. However, the 2-RDM is not necessarily N-representable. While derived without the wave function, this parametrization of the 2-RDM is essentially equivalent to the coupled electron pair approximation, known as CEPA0. As in ref 91, it can be readily extended to include single excitations.

4.2. *N*-Representability of the 2-RDM

The most important N-representability conditions are the 2-positivity conditions. The 2-positivity conditions imply N-representability conditions known as the *Cauchy−Schwarz inequalities*. From nonnegativity of ${}^2D$ and ${}^2Q$, we have

$$ ({}^2D^{ij}_{ab})^2 \le {}^2D^{ij}_{ij}\,{}^2D^{ab}_{ab} \quad (57) $$

$$ ({}^2Q^{ij}_{ab})^2 \le {}^2Q^{ij}_{ij}\,{}^2Q^{ab}_{ab} \quad (58) $$

These inequalities become equalities in two cases: (i) when correlation is absent, both sides of the inequalities trivially vanish, and (ii) when the number of particles (holes) equals two, eq 57 (eq 58) becomes an equality. Equation 57 (eq 58) is an inequality mainly due to unconnected terms (terms scaling as N^p where $p \ge 2$) that appear on the right side when the number of particles (holes) is greater than two.

Substituting the definitions of the 2-RDM elements into these inequalities and equating the connected parts on each side gives parametrizations of the cumulant 2-RDM elements ${}^2\Delta^{ab}_{ij}$ that improve the 2-RDM's N-representability.[83,91] Taking different averages of the six size extensive equations yields a family of 2-RDM parametrizations including those introduced by Kollmar[84,85] and Mazziotti.[83,91] The general family of 2-RDM parametrizations can be expressed as

$$ {}^2\Delta^{ab}_{ij} = {}^2T^{ab}_{ij}\sqrt{1-\frac{1}{4}\sum_{cdkl} f^{abcd}_{ijkl}\,|{}^2T^{cd}_{kl}|^2} \quad (59) $$

where the values of f^{abcd}_{ijkl}, known as the topological factor, for different parametrizations are given in Table 1. Because a topological factor f^{ijkl}_{abcd} only depends on the number of indices shared by ${}^2T^{ab}_{ij}$ and ${}^2T^{cd}_{kl}$ in eq 59, its possible values can be divided into nine classes, labeled by n_o/n_v, where n_o is the number of occupied orbitals shared by $\{ij\}$ and $\{kl\}$ and n_v is the number of virtual orbitals shared by $\{ab\}$ and $\{cd\}$. For the energy functional to be size extensive, the topological factor must vanish for the class $n_o/n_v = 0/0$. Table 1 defines the elements of the topological factors for CID and CEPA as well as those corresponding to the parametrizations of Kollmar (K) and Mazziotti (M). The derivation here can be extended to the case where non-zero single-excitation coefficients contribute to the 1- and 2-RDM elements.[91]

Table 1. Elements of the Topological Factors for CID, CEPA, and the D, Q, K, and M Parametric 2-RDM Methods Defined.[a]

	topological factors, f^{ijkl}_{abcd} (or f_{n_o/n_v})								
2-RDM methods	0/0	1/0	2/0	0/1	0/2	1/1	2/1	1/2	2/2
CID	1	1	1	1	1	1	1	1	1
CEPA	0	0	0	0	0	0	0	0	0
D	0	1	1	0	0	1	1	1	1
Q	0	0	0	1	1	1	1	1	1
K	0	1/2	1	1/2	1	3/4	1	1	1
M	0	0	1	0	1	1	1	1	1

[a] Reprinted with permission from ref 83. Copyright 2008 American Physical Society.

Table 2. Correlation Energies from Parametric 2-RDM Methods as well as Traditional Wavefunction Methods for Molecules in the cc-pVQZ Basis Set except for NH_3 and HCN in the cc-pVTZ Basis Set[a]

		correlation energy				
		wave function methods		2-RDM methods		
molecules	HF energy	CCSD	CCSD(T)	CISD	K	M
H_2O	−76.0648	−0.2860	−0.2950	−0.2744	−0.2868	−0.2904
CH_2	−38.8947	−0.1712	−0.1765	−0.1647	−0.1729	−0.1761
N_2	−108.9911	−0.3931	−0.4133	−0.3657	−0.3957	−0.4032
CO	−112.7888	−0.3805	−0.3990	−0.3556	−0.3837	−0.3906
NH_3	−56.2179	−0.2476	−0.2553	−0.2368	−0.2487	−0.2522
HCN	−92.9081	−0.3492	−0.3671	−0.3237	−0.3518	−0.3586

[a] The M 2-RDM methods improve significantly upon CCSD. All energies are given in hartrees.

4.3. Applications

To illustrate the parametric 2-RDM methods, we examine correlation energies of several molecules at equilibrium,[83,91] the dissociation of hydrogen fluoride,[91] and applications to the isomerization of nitrosomethane[90] and the conversion of oxywater to hydrogen peroxide.

4.3.1. Correlation Energies at Equilibrium Geometries.

Correlation energies from parametric 2-RDM methods as well as traditional wave function methods are reported in Table 2 for several molecules in the polarized quadruple-ζ (cc-pVQZ) basis set.[91,150] Molecules NH_3 and HCN are given in the correlation-consistent polarized triple-ζ (cc-pVTZ) basis set.[150] The K and M methods recover much more correlation energy than CISD, which is not size extensive. Furthermore, the M method

dx.doi.org/10.1021/cr2000493 |Chem. Rev. 2012, 112, 244–262

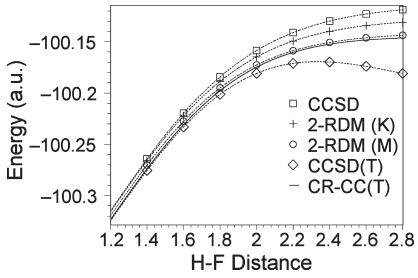

Figure 17. The potential energy curves for hydrogen fluoride in the cc-pVQZ basis set from the K, M, CCSD, CCSD(T), and CR-CC(2,3) methods. The energy results of the M functional are nearly indistinguishable from those of the computationally more expensive CR-CC-(2,3). The length of the H−F bond is given in angstroms (Å). Reprinted with permission from ref 91. Copyright 2010 American Physical Society.

improves significantly upon CCSD with energies that are closer to those from CCSD(T). The K method improves slightly upon CCSD. The 2-RDMs from the parametric methods are nearly *N*-representable; for example, with the M method for N_2 the lowest eigenvalues of ^2D, ^2Q, and ^2G, -5.0×10^{-4}, -3.0×10^{-4}, and -4.1×10^{-4}, are 3−4 orders of magnitude smaller than the largest eigenvalues.

4.3.2. Dissociation of the HF Molecule. In Figure 17, the dissociation curve for hydrogen fluoride is presented in a cc-pVQZ basis set.[91,150] Because FCI calculations are not available for such a large basis set, we compare the energy errors from the K, M, and M_2 parametric 2-RDM methods and the CCSD and CCSD(T) coupled-cluster methods relative to the energies from the completely renormalized coupled cluster method with perturbative triple excitations [CR-CC(2,3)].[151] Both CCSD(T) and CR-CC(2,3), scaling approximately as r^7, contain a perturbative treatment of triple excitations. For hydrogen fluoride at 2.8 Å, the CCSD, CCSD(T), K, and M methods yield energy errors of 27.5, −34.6, 15.3, and 2.6 mhartree, respectively. Furthermore, the NPEs from CCSD, CCSD(T), K, and M are 19.1, −33.4, 7.8, and 2.1 mhartree. The M functional performs better in this basis set than in the smaller 6-311G** basis set. Figure 17 displays the potential energy curves for hydrogen fluoride from the K, M, CCSD, CCSD(T), and CR-CC(2,3) methods. The energy results of the M functional are nearly indistinguishable from those of the computationally more expensive CR-CC(2,3)

4.3.3. Isomerization of Nitrosomethane. The parametric 2-RDM method with the K parametrization was recently applied to the isomerization of nitrosomethane to *trans*-formaldoxime, which can occur by (i) a single 1,3-hydrogen shift or (ii) two successive 1,2-hydrogen shifts.[90] The potential energy surface from the 2-RDM method with the K functional in the aug-cc-pVTZ basis set is shown in Figure 18 where we present energies in kcal/mol of the stationary points relative to nitrosomethane. Because the parametric 2-RDM method minimizes the energy with respect to its parameters, the first derivative of the ground-state energy with respect to an arbitrary nuclear coordinate *depends only on the derivatives of the one- and two-electron integrals.* Hence, geometry optimization can be efficiently implemented with one evaluation of the parametric 2-RDM method for each gradient update of the molecular geometry as discussed in ref 88. The solid line follows the channel describing successive 1,2-hydrogen shifts, while the dashed line follows a single 1,3-hydrogen shift to *cis*-formaldoxime followed by a rotation with a barrier of about 3 kcal/mol to *trans*-formaldoxime, which is globally the lowest energy species on the surface. We note that the barrier of the 1,3-shift is slightly higher than the barrier of the first 1,2-shift, with heights relative to nitrosomethane of 65.0 and 55.2 kcal/mol, respectively, as predicted by the 2-RDM method.

4.3.4. Kinetic Stability of Oxywater. Recently, the parametric 2-RDM method with the K and M parametrization was applied to computing the activation energy for the conversion of oxywater to hydrogen peroxide. The potential energy curve for the reaction of oxywater (OW) to hydrogen peroxide (HP) is shown in Figure 19 in the extrapolated basis-set limit (EBSL). (Also displayed is the dissociation of hydrogen peroxide into two hydroxyl radicals.) In the EBSL, the CCSD, CR-CC(T), and CCSD(T) methods predict the energy of the transition state (TS) relative to OW to be 6.6, 5.1, and 4.5 kcal/mol, respectively, while the K and M parametric 2-RDM methods predict activation energies of 5.0 and 2.2 kcal/mol, respectively. While the activation energy of 3.6 kcal/mol from CCSD(T) in the aug-cc-pVTZ basis set agrees with the barriers of 3.3 and 3.9 kcal/mol obtained previously in similar triple-ζ basis sets,[152,153] the activation energy from CCSD(T) in the aug-cc-pVQZ basis set, containing *twice* as many basis functions, is 4.0 kcal/mol, which leads to the 4.5 kcal/mol in the extrapolated limit. Importantly, the M parametric 2-RDM method predicts a lower barrier of 2.2 kcal/mol in the basis-set limit. The M functional has been shown to be especially effective in treating the multi-reference electron correlation in hydrogen abstraction and non-equilibrium geometries such as transition states. Hence, it is reasonable that the energy from the M functional lies between the CCSD(T) energy and earlier CASPT2 energies, which predicted small or nonexistent barriers.[153]

5. FUTURE DIRECTIONS

The collection of 2-RDM methods offers a new paradigm for the computation of electron correlation in quantum systems.[7] While the wave function scales exponentially in the number *N* of electrons, the 2-RDM scales polynomially in *N*. Consequently, for many-electron quantum systems, the 2-RDM theory offers a significant reduction in computational cost even in the presence of strong electron correlation. The 2-RDM has long been employed as a tool for analysis of quantum information, but as discussed in the Introduction, efforts to compute the 2-RDM directly were hindered by the *N*-representability problem, that is, the 2-RDM must be constrained to correspond to an *N*-electron system.[11]

Recent advances[7] have enabled the direct computation of the 2-RDM without the many-electron wave function by the methods discussed in this review: (i) the constrained and parametric variational 2-RDM methods and (ii) the solution of the contracted Schrödinger equation or its anti-Hermitian part. Importantly, as seen with the acene chains[78] and the hydrogen lattices,[81] these 2-RDM approaches permit the treatment of strong electron correlation in systems that are too large to treat with traditional electronic structure methods. The variational 2-RDM method is applicable to a broader range of molecules including systems lacking a clear ordering of orbitals by space or energy, which can be challenging for density-matrix renormalization group.[154] The 2-RDM-based methods have been applied to study: (i) chemical reactions and materials,[47−53,78,80,81,89,90] (ii) quantum phase transitions,[101,102] (iii) motions of electrons and nuclei,[79,38,103] (iv) molecular conductivity,[155,156] and (v) high-temperature superconductivity.[157]

dx.doi.org/10.1021/cr2000493 |*Chem. Rev.* 2012, 112, 244–262

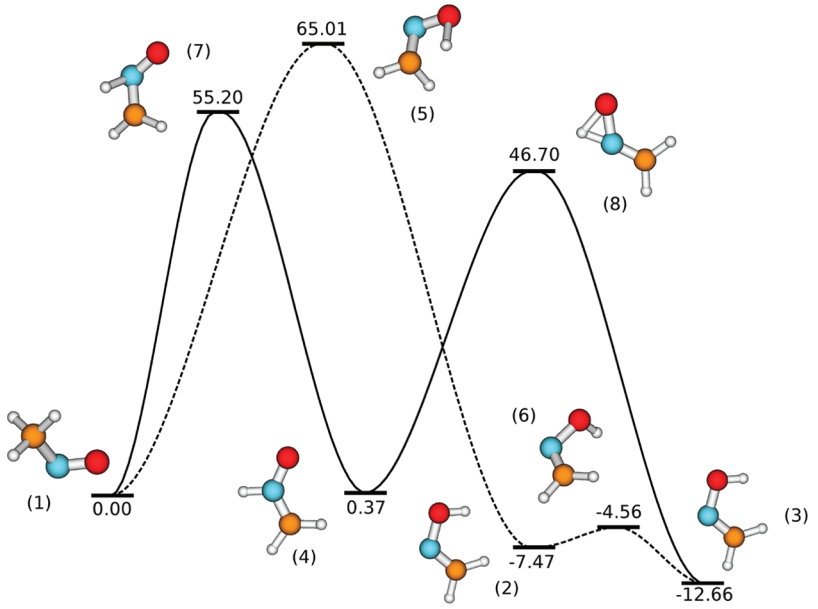

Figure 18. Critical points on the potential energy surface for the isomerization of nitrosomethane to *trans*-formaldoxime as computed by the 2-RDM method in the aug-cc-pVTZ basis set. The dashed line represents a 1,3-hydrogen shift; the solid line represents successive 1,2-shifts. The figure shows that the 1,2-shift is energetically more favorable than the 1,3-shift by about 10 kcal/mol. Reprinted with permission from ref 90. Copyright 2010 American Institute of Physics.

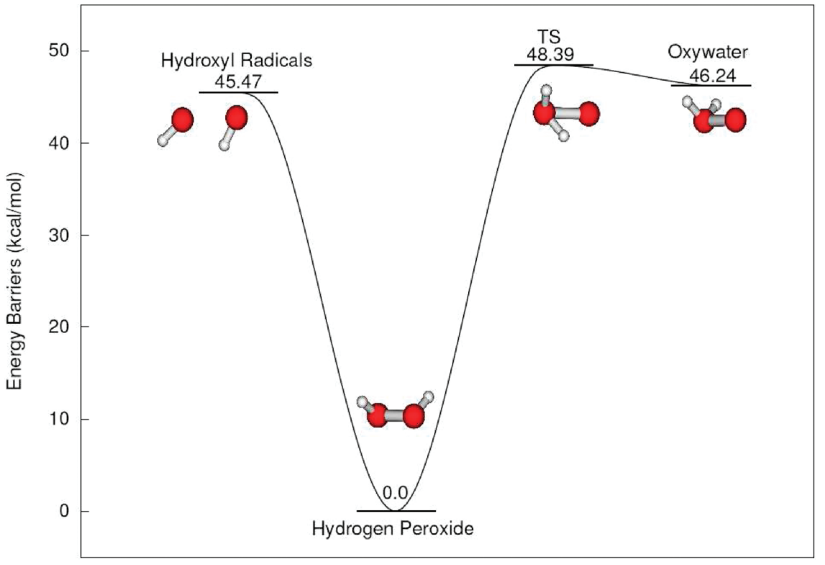

Figure 19. Reaction and activation energies for the conversion of hydrogen peroxide (HP) to (i) oxywater (OX) and (ii) two hydroxyl radicals (HR) are shown schematically from the M parametric 2-RDM method in the extrapolated basis-set limit. The M activation energy of 2.2 kcal/mol from OX to HP is smaller than the energies from coupled cluster methods and larger than the energy from complete active-space second-order perturbation theory. Reprinted with permission from ref 99. Copyright 2011 American Institute of Physics.

While significant progress has been made, there remain many important opportunities for further advancements in theory and applications. A sampling of future extensions of recent work might include: (i) improvements in the computational efficiency of the first-order semidefinite-programming algorithms,[64,65,77] (ii) enhancements of existing linear-scaling parametric 2-RDM methods[89] for the better treatment of medium-to-large molecular systems, and (iii) generalizations of existing nonequilibrium steady-state ACSE methods[155,156] to treat electron correlation in molecular conductors explicitly. It is hoped that the present review may serve as a starting point for these and other new developments in 2-RDM mechanics that will further enhance our ability to study and understand quantum molecular systems and processes.

AUTHOR INFORMATION

Corresponding Author

*Electronic address: damazz@uchicago.edu.

BIOGRAPHY

The author received his Bachelor's degree in Chemistry from Princeton University in 1995 and a Ph.D. in Chemical Physics from Harvard University in 1999. He then performed postdoctoral research at Duke University and Princeton University. From 2002 to the present time, he has been on the faculty of The University of Chicago in the Department of Chemistry and The James Franck Institute. He has been awarded the Alfred P. Sloan Fellowship, the David and Lucile Packard Fellowship in Science and Engineering, the Camille and Henry Dreyfus Teacher-Scholar Award, and the Microsoft Newton Award. Professor Mazziotti's research interests lie at the intersection of chemistry, physics, biology, and applied mathematics with special interest in advanced molecular electronic structure and quantum dynamics and control.

ACKNOWLEDGMENT

The author expresses his appreciation to Dudley Herschbach, Herschel Rabitz, and Alexander Mazziotti for their support and encouragement. He thanks the members of his research group, past and present, who have contributed to the development of 2-RDM methods. Finally, the author also gratefully acknowledges the NSF (No. CHE-644888), the ARO, the Henry-Camille Dreyfus Foundation, the Alfred P. Sloan Foundation, Microsoft Corporation, and the David-Lucile Packard Foundation for their support.

REFERENCES

(1) Schrödinger, E. *Phys. Rev.* **1926**, *28*, 1049.
(2) Eyring, H.; Walter, J.; Kimball, G. *Quantum Chemistry*; John Wiley and Sons: New York, 1944.
(3) Roothaan, C. C. J. *Rev. Mod. Phys.* **1951**, *23*, 69.
(4) Hehre, W. J.; Stewart, R. F.; Pople, J. A. *J. Chem. Phys.* **1969**, *51*, 2657.
(5) Crawford, T. D.; Schaefer, H. F., III *Rev. Comput. Chem.* **2000**, *14*, 33.
(6) Parr, R. G.; Yang, W. *Density Functional Theory of Atoms and Molecules*; Oxford University Press: New York, 1994.
(7) *Reduced-Density-Matrix Mechanics: With Application to Many-Electron Atoms and Molecules*; Mazziotti, D. A., Ed.; Wiley: New York, 2007; Vol. 134.
(8) Coleman, A. J.; Yukalov, V. I. *Reduced Density Matrices: Coulson's Challenge*; Springer-Verlag: New York, 2000.
(9) Mayer, J. E. *Phys. Rev.* **1955**, *100*, 1579.
(10) Löwdin, P. O. *Phys. Rev.* **1955**, *97*, 1474.
(11) Coleman, A. J. *Rev. Mod. Phys.* **1963**, *35*, 668.
(12) Tredgold, R. H. *Phys. Rev.* **1957**, *105*, 1421.
(13) Mihailovic¢, M. V.; Rosina, M. *Nucl. Phys.* **1975**, *A237*, 221.
(14) Garrod, C.; Mihailovic¢, V.; Rosina, M. *J. Math. Phys.* **1975**, *10*, 1855.
(15) Erdahl, R. M. *Rep. Math. Phys.* **1979**, *15*, 147.
(16) Colmenero, F.; del Valle, C. P.; Valdemoro, C. *Phys. Rev. A* **1993**, *47*, 971.
(17) Colmenero, F.; Valdemoro, C. *Phys. Rev. A* **1993**, *47*, 979.
(18) Colmenero, F.; Valdemoro, C. *Int. J. Quantum Chem.* **1994**, *51*, 369.
(19) Nakatsuji, H.; Yasuda, K. *Phys. Rev. Lett.* **1996**, *76*, 1039.
(20) Yasuda, K.; Nakatsuji, H. *Phys. Rev. A* **1997**, *56*, 2648.
(21) Mazziotti, D. A. *Phys. Rev. A* **1998**, *57*, 4219.
(22) Mazziotti, D. A. *Chem. Phys. Lett.* **1998**, *289*, 419.
(23) Mazziotti, D. A. *Int. J. Quantum Chem.* **1998**, *70*, 557.
(24) Mazziotti, D. A. *Phys. Rev. A* **1999**, *60*, 3618.
(25) Mazziotti, D. A. *Phys. Rev. A* **1999**, *60*, 4396.
(26) Kutzelnigg, W.; Mukherjee, D. *J. Chem. Phys.* **1999**, *110*, 2800.
(27) Yasuda, K. *Phys. Rev. A* **1999**, *59*, 4133.
(28) Mazziotti, D. A. *Chem. Phys. Lett.* **2000**, *326*, 212.
(29) Mazziotti, D. A. In *Many-Electron Densities and Density Matrices*; Cioslowski, J., Ed.; Kluwer: Boston, 2000.
(30) Kutzelnigg, W.; Mukherjee, D. *J. Chem. Phys.* **2001**, *114*, 2047.
(31) Mazziotti, D. A. *J. Chem. Phys.* **2002**, *116*, 1239.
(32) Benayoun, M. D.; Lu, A. Y.; Mazziotti, D. A. *Chem. Phys. Lett.* **2004**, *387*, 485.
(33) Alcoba, D. R.; Casquero, F. J.; Tel, L. M.; Perez-Romero, E.; Valdemoro, C. *Int. J. Quantum Chem.* **2005**, *102*, 620.
(34) Valdemoro, C. In *Reduced-Density-Matrix Mechanics with Application to Many-Electron Atoms and Molecules*; Mazziotti, D. A., Ed.; John Wiley and Sons: New York, 2007; Vol. 134, p 121.
(35) Alcoba, D. In *Reduced-Density-Matrix Mechanics with Application to Many-Electron Atoms and Molecules*; Mazziotti, D. A., Ed.; John Wiley and Sons: New York, 2007; Vol. 134, p 205.
(36) Mazziotti, D. A. In *Reduced-Density-Matrix Mechanics with Application to Many-Electron Atoms and Molecules*; Mazziotti, D. A., Ed.; John Wiley and Sons: New York, 2007; Vol. 134, p 165.
(37) Herbert, J.; Harriman, J. E. In *Reduced-Density-Matrix Mechanics with Application to Many-Electron Atoms and Molecules*; Mazziotti, D. A., Ed.; John Wiley and Sons: New York, 2007; Vol. 134, p 261.
(38) Kamarchik, E.; Mazziotti, D. A. *Phys. Rev. A* **2007**, *75*, No. 013203.
(39) Mazziotti, D. A. *Phys. Rev. Lett.* **2006**, *97*, No. 143002.
(40) Mazziotti, D. A. In *Reduced-Density-Matrix Mechanics with Application to Many-Electron Atoms and Molecules*; Mazziotti, D. A., Ed.; John Wiley and Sons: New York, 2007; Vol. 134, p 331.
(41) Mazziotti, D. A. *Phys. Rev. A* **2007**, *75*, No. 022505.
(42) Mazziotti, D. A. *J. Chem. Phys.* **2007**, *126*, No. 184101.
(43) Valdemoro, C.; Tel, L. M.; Alcoba, D. R.; Pérez-Romero, E. *Theor. Chem. Acc.* **2007**, *118*, No. 503509.
(44) Mazziotti, D. A. *J. Phys. Chem. A* **2007**, *111*, 12635.
(45) Mazziotti, D. A. *Phys. Rev. A* **2007**, *76*, No. 052502.
(46) Valdemoro, C.; Tel, L. M.; Pérez-Romero, E.; Alcoba, D. R. *Int. J. Quantum Chem.* **2008**, *108*, 1090.
(47) Mazziotti, D. A. *J. Phys. Chem. A* **2008**, *112*, 13684.
(48) Foley, J. J., IV; Rothman, A. E.; Mazziotti, D. A. *J. Chem. Phys.* **2009**, *130*, No. 184112.
(49) Valdemoro, C.; Alcoba, D. R.; Tel, L. M.; Pérez-Romero, E. *Int. J. Quantum Chem.* **2009**, *109*, 2622.
(50) Gidofalvi, G.; Mazziotti, D. A. *Phys. Rev. A* **2009**, *80*, No. 022507.
(51) Rothman, A. E.; Foley, J. J., IV; Mazziotti, D. A. *Phys. Rev.A* **2009**, *80*, No. 052508.
(52) Greenman, L.; Mazziotti, D. A. *J. Phys. Chem. A* **2010**, *114*, 583.
(53) Snyder, J. W., Jr.; Rothman, A. E.; Foley, J. J., IV; Mazziotti, D. A. *J. Chem. Phys.* **2010**, *132*, No. 154109.
(54) Foley, J. J., IV; Mazziotti, D. A. *Mol. Phys.* **2010**, *108*, 2543.
(55) Rothman, J. J. F. A. E.; Mazziotti, D. A. *J. Chem. Phys.* **2011**, *134*, No. 034111.

(56) Mazziotti, D. A.; Erdahl, R. M. *Phys. Rev. A* **2001**, *63*, No. 042113.
(57) Nakata, M.; Nakatsuji, H.; Ehara, M.; Fukuda, M.; Nakata, K.; Fujisawa, K. *J. Chem. Phys.* **2001**, *114*, 8282.
(58) Mazziotti, D. A. *Phys. Rev. A* **2002**, *65*, No. 062511.
(59) Nakata, M.; Ehara, M.; Nakatsuji, H. *J. Chem. Phys.* **2002**, *116*, 5432.
(60) Mazziotti, D. A. *Phys. Rev. A* **2002**, *66*, No. 062503.
(61) Gidofalvi, G.; Mazziotti, D. A. *Phys. Rev. A* **2004**, *69*, No. 042511.
(62) Juhász, T.; Mazziotti, D. A. *J. Chem. Phys.* **2004**, *121*, 1201.
(63) Zhao, Z.; Braams, B. J.; Fukuda, H.; Overton, M. L.; Percus, J. K. *J. Chem. Phys.* **2004**, *120*, 2095.
(64) Mazziotti, D. A. *Phys. Rev. Lett.* **2004**, *93*, No. 213001.
(65) Mazziotti, D. A. *J. Chem. Phys.* **2004**, *121*, 10957.
(66) Gidofalvi, G.; Mazziotti, D. A. *J. Chem. Phys.* **2005**, *122*, No. 094107.
(67) Gidofalvi, G.; Mazziotti, D. A. *J. Chem. Phys.* **2005**, *122*, No. 194104.
(68) Gidofalvi, G.; Mazziotti, D. A. *Phys. Rev. A* **2005**, *72*, No. 052505.
(69) Mazziotti, D. A. *Phys. Rev. A* **2005**, *72*, No. 032510.
(70) Hammond, J. R.; Mazziotti, D. A. *Phys. Rev. A* **2006**, *73*, No. 012509.
(71) Mazziotti, D. A. *Acc. Chem. Res.* **2006**, *39*, 207.
(72) Gidofalvi, G.; Mazziotti, D. A. *J. Phys. Chem. A* **2006**, *110*, 5481.
(73) Mazziotti, D. A. *Phys. Rev. A* **2006**, *74*, No. 032501.
(74) Gidofalvi, G.; Mazziotti, D. A. *J. Chem. Phys.* **2007**, *126*, No. 024105.
(75) Nakata, M.; Braams, B. J.; Fujisawa, K.; Fukuda, M.; Percus, J. K.; Yamashita, M.; Zhao, Z. *J. Chem. Phys.* **2008**, *128*, No. 164113.
(76) Mazziotti, D. A. In *Reduced-Density-Matrix Mechanics with Application to Many-Electron Atoms and Molecules*; Mazziotti, D. A., Ed.; John Wiley and Sons: New York, 2007; Vol. 134, p 21.
(77) Mazziotti, D. A. *Math. Modell. Numer. Anal.* **2007**, *41*, 249.
(78) Gidofalvi, G.; Mazziotti, D. A. *J. Chem. Phys.* **2008**, *129*, No. 134108.
(79) Kamarchik, E.; Mazziotti, D. A. *Phys. Rev. A* **2009**, *79*, No. 012502.
(80) Greenman, L.; Mazziotti, D. A. *J. Chem. Phys.* **2009**, *130*, No. 184101.
(81) Sinitskiy, A. V.; Greenman, L.; Mazziotti, D. A. *J. Chem. Phys.* **2010**, *133*, No. 014104.
(82) Jin, B. Y. Ph.D. thesis, Department of Mathematics and Statistics,Queen's University, 1998
(83) Mazziotti, D. A. *Phys. Rev. Lett.* **2008**, *101*, No. 253002.
(84) Kollmar, C. *J. Chem. Phys.* **2006**, *125*, No. 084108.
(85) DePrince, A. E., III; Mazziotti, D. A. *Phys. Rev. A.* **2007**, *76*, No. 042501.
(86) DePrince, A. E., III; Kamarchik, E.; Mazziotti, D. A. *J. Chem. Phys.* **2008**, *128*, 234103.
(87) DePrince, A. E., III; Mazziotti, D. A. *J. Phys. Chem. B* **2008**, *112*, 16158.
(88) DePrince, A. E., III; Mazziotti, D. A. *J. Chem. Phys.* **2009**, *130*, No. 164109.
(89) DePrince, A. E., III; Mazziotti, D. A. *J. Chem. Phys.* **2010**, *132*, No. 034110.
(90) DePrince, A. E., III; Mazziotti, D. A. *J. Chem. Phys.* **2010**, *133*, No. 034112.
(91) Mazziotti, D. A. *Phys. Rev. A* **2010**, *81*, No. 062515.
(92) Erdahl, R. M. In *Reduced-Density-Matrix Mechanics with Application to Many-Electron Atoms and Molecules*; Mazziotti, D. A., Ed.; John Wiley and Sons: New York, 2007; Vol. 134, p 61.
(93) Braams, B. J.; Percus, J. E.; Zhao, Z. In *Reduced-Density-Matrix Mechanics with Application to Many-Electron Atoms and Molecules*; Mazziotti, D. A., Ed.; John Wiley and Sons: New York, 2007; Vol. 134, p 93.
(94) Fukuda, M.; Nakata, M.; Yamashita, M. In *Reduced-Density-Matrix Mechanics with Application to Many-Electron Atoms and Molecules*; Mazziotti, D. A., Ed.; John Wiley and Sons: New York, 2007; Vol. 134, p 103.
(95) Nakata, M.; Yasuda, K. *Phys. Rev. A* **2009**, *80*, No. 042109.
(96) van Aggelen, H.; Verstichel, B.; Bultinck, P.; Neck, D. V.; Ayers, P. W.; Cooper, D. L. *J. Chem. Phys.* **2010**, *132*, No. 114112.
(97) Verstichel, B.; van Aggelen, H.; Neck, D. V.; Ayers, P. W.; Bultinck, P. *J. Chem. Phys.* **2010**, *132*, No. 114113.
(98) Shenvi, N.; Izmaylov, A. *Phys. Rev. Lett.* **2010**, *105*, No. 213003.
(99) Schwerdtfeger, C. A.; DePrince, A. E., III; Mazziotti, D. A. *J. Chem. Phys.* **2011**, *134*, No. 174102.
(100) Greenman, L.; Mazziotti, D. A. *J. Chem. Phys.* **2010**, *133*, No. 164110.
(101) Gidofalvi, G.; Mazziotti, D. A. *Phys. Rev. A* **2006**, *74*, No. 012501.
(102) Schwerdtfeger, C. A.; Mazziotti, D. A. *J. Chem. Phys.* **2009**, *130*, No. 224102.
(103) Kamarchik, E.; Mazziotti, D. A. *Phys. Rev. Lett.* **2007**, *99*, No. 243002.
(104) Pelzer, K.; Greenman, L.; Gidofalvi, G.; Mazziotti, D. A. *J.Phys. Chem. A* **2011**, *115*, 5632.
(105) Nakatsuji, H. *Phys. Rev. A* **1976**, *14*, 41.
(106) Harriman, J. E. *Phys. Rev. A* **1979**, *19*, 1893.
(107) Cohen, L.; Frishberg, C. *Phys. Rev. A* **1976**, *13*, 927.
(108) Kutzelnigg, W. *Chem. Phys. Lett.* **1979**, *64*, 383.
(109) Hirschfelder, J. O. *J. Chem. Phys.* **1960**, *33*, 1462.
(110) DePrince, A. E., III; Mazziotti, D. A. *J. Chem. Phys.* **2007**, *127*, No. 104104.
(111) Slebodzinski, W. *Exterior Forms and their Applications*; Polish Scientific Publishers: Warsaw, 1970.
(112) Yanai, T.; Chan, G. K. *J. Chem. Phys.* **2006**, *124*, No. 194106.
(113) Chan, G. K.; Yanai, T. In *Reduced-Density-Matrix Mechanics: With Application to Many-Electron Atoms and Molecules*; Mazziotti, D. A., Ed.; Wiley: New York, 2007; Vol. 134, p 343.
(114) Yarkony, D. R. *Rev. Mod. Phys.* **1996**, *68*, 4.
(115) Turro, N. J. *Modern Molecular Photochemistry*; University Science Books: Sausalito, CA, 1991.
(116) Garrod, C.; Percus, J. *J. Math. Phys.* **1964**, *5*, 1756.
(117) Erdahl, R. M.; Jin, B. In *Many-Electron Densities and Density Matrices*; Cioslowski, J., Ed.; Kluwer: Boston, 2000.
(118) Erdahl, R. M. *Int. J. Quantum Chem.* **1978**, *13*, 697.
(119) Vandenberghe, L.; Boyd, S. *SIAM Rev.* **1996**, *38*, 49.
(120) Mazziotti, D. A. *Phys. Rev. E* **2002**, *65*, No. 026704.
(121) Hammond, J. R.; Mazziotti, D. A. *Phys. Rev. A* **2005**, *71*, No. 062503.
(122) Wright, S. *Primal-Dual Interior-Point Methods*; SIAM: Philadelphia, PA, 1997.
(123) Nesterov, Y.; Nemirovskii, A. S. *Interior Point Polynomial Method in Convex Programming: Theory and Applications*; SIAM: Philadelphia, PA, 1993.
(124) Mihailovic, M. V.; Rosina, M. *Nucl. Phys.* **1969**, *A130*, 386.
(125) Harriman, J. E. *Phys. Rev. A* **1978**, *17*, 1257.
(126) Burer, S.; Monteiro, R. D. C. *Math. Program., Ser. B* **2003**, *95*, 329.
(127) Burer, S.; Choi, C. *Optim. Methods Software* **2006**, *21*, 493.
(128) Fletcher, R. *Practical Methods of Optimization*; John Wiley and Sons: New York, 1987.
(129) Cancés, E.; Stoltz, G.; Lewin, M. *J. Chem. Phys.* **2006**, *125*, No. 064101.
(130) Verstichel, B.; van Aggelen, H.; Neck, D. V.; Ayers, P. W.; Bultinck, P. *Phys. Rev. A* **2009**, *80*, No. 032508.
(131) Mazziotti, D. A. *Phys. Rev. Lett.* **2011**, *106*, 083001.
(132) Chung, L. W.; Hayashi, S.; Lundberg, M.; Nakatsu, T.; Kato, H.; Morokuma, K. *J. Am. Chem. Soc.* **2008**, *130*, 12880.
(133) Liu, F. Y.; Liu, Y. J.; Vico, L. D.; Lindh, R. *J. Am. Chem. Soc.* **2009**, *131*, 6181.
(134) Juhasz, T.; Mazziotti, D. A. *J. Chem. Phys.* **2006**, *125*, No. 174105.
(135) Huang, Z.; Kais, S. *Chem. Phys. Lett.* **2005**, *413*, 1.

(136) Kais, S. In *Reduced-Density-Matrix Mechanics with Application to Many-Electron Atoms and Molecules*; Mazziotti, D. A., Ed.; John Wiley and Sons: New York, 2007; Vol. 134, p 493.
(137) Wales, D. J. *Energy Landscapes*; Cambridge University Press: Cambridge, U.K., 2003.
(138) Skone, J. H.; Pak, M. V.; Hammes-Schiffer, S. *J. Chem. Phys.* **2005**, *123*, No. 134108.
(139) Chakraborty, A.; Hammes-Schiffer, S. *J. Chem. Phys.* **2008**, *129*, No. 204101.
(140) Rowe, W. F.; Duerst, R. W.; Wilson, E. B. *J. Am. Chem. Soc.* **1976**, *98*, 4021.
(141) Fillaux, F.; Nicolaï, B. *Chem. Phys. Lett.* **2005**, *415*, 357.
(142) Sachdev, S. *Quantum Phase Transitions*; Cambridge University Press: New York, 1999.
(143) Lipkin, H. J.; Meshkov, N.; Glick, A. J. *Nucl. Phys.* **1965**, *62*, 188.
(144) Pfeuty, P. *Ann. Phys.* **1970**, *57*, 79.
(145) Verstraete, F.; Cirac, J. I. *Phys. Rev. B* **2006**, *73*, No. 094423.
(146) Piris, M. In *Reduced-Density-Matrix Mechanics with Application to Many-electron Atoms and Molecules*; Mazziotti, D. A., Ed.; John Wiley and Sons: New York, 2007; Vol. 134, p 387.
(147) Piris, M.; Matxain, J. M.; Lopez, X.; Ugalde, J. M. *J. Chem. Phys.* **2010**, *133*, No. 111101.
(148) Harriman, J. E. *Phys. Rev. A* **2007**, *75*, No. 032513.
(149) Nesbet, R. K. *Phys. Rev.* **1958**, *109*, 1632.
(150) Dunning, T. H. *J. Chem. Phys.* **1989**, *90*, 1007.
(151) Piecuch, P.; Wloch, M. *J. Chem. Phys.* **2005**, *123*, No. 224105.
(152) Huang, H. H.; Xie, Y.; Schaefer, H. F., III *J. Phys. Chem.* **1996**, *100*, 6076.
(153) Ge, Y.; Olsen, K.; Kaiser, R. I.; Head, J. D. In *Astrochemistry: From Laboratory Studies to Astronomical Observations*; Kaiser, R. I., Bernath, P., Osamura, Y., Petrie, S., Mebel, A. M., Eds.; American Institute of Physics: New York, 2006.
(154) Hachmann, J.; Cardoen, W.; Chan, G. K. *J. Chem. Phys.* **2006**, *125*, No. 144101.
(155) Subotnik, J. E.; Hansen, T.; Ratner, M. A.; Nitzan, A. *J. Chem. Phys.* **2009**, *130*, No. 144105.
(156) Rothman, A. E.; Mazziotti, D. A. *J. Chem. Phys.* **2010**, *132*, No. 104112.
(157) Phillips, J. C. *Proc. Natl. Acad. Sci. U.S.A.* **2010**, *107*, 1307.